



HAL
open science

Blood transcriptome changes linked to long-term arsenic exposure through drinking water – a cross-sectional study from the Bolivian Andes

Ying Yang, Anastasiia Snigireva, Jessika Barron, Noemi Tirado, Maria Teresa Alvarez Aliaga, Gina Torres, Paolo Manghi, Philippe Gérard, Michael Levi, Jacques Gardon, et al.

► To cite this version:

Ying Yang, Anastasiia Snigireva, Jessika Barron, Noemi Tirado, Maria Teresa Alvarez Aliaga, et al.. Blood transcriptome changes linked to long-term arsenic exposure through drinking water – a cross-sectional study from the Bolivian Andes. *Environment International*, 2025, 203, pp.109727. <10.1016/j.envint.2025.109727>. <hal-05215138>

HAL Id: hal-05215138

<https://hal.science/hal-05215138v1>

Submitted on 19 Aug 2025

HAL is a multi-disciplinary open access archive for the deposit and dissemination of scientific research documents, whether they are published or not. The documents may come from teaching and research institutions in France or abroad, or from public or private research centers.

L'archive ouverte pluridisciplinaire HAL, est destinée au dépôt et à la diffusion de documents scientifiques de niveau recherche, publiés ou non, émanant des établissements d'enseignement et de recherche français ou étrangers, des laboratoires publics ou privés.








Distributed under a Creative Commons CC BY 4.0 - Attribution - International License



Full length article

Blood transcriptome changes linked to long-term arsenic exposure through drinking water – a cross-sectional study from the Bolivian Andes

Ying Yang^a, Anastasiia Snigireva^{a,1} , Jessika Barron^{b,1} , Noemi Tirado^{b,d},
 Maria Teresa Alvarez Aliaga^c, Gina Torres^b, Paolo Manghi^e, Philippe Gérard^f , Michael Levi^a,
 Jacques Gardon^g , Harri Alenius^{a,*} , Karin Broberg^a

^a Institute of Environmental Medicine, Karolinska Institutet, Stockholm, Sweden

^b Genetics Institute, Universidad Mayor de San Andrés, La Paz, Bolivia

^c Instituto de Investigaciones Fármaco Bioquímicas, Universidad Mayor de San Andrés, La Paz, Bolivia

^d Academia Nacional de Ciencias de Bolivia, Bolivia

^e Research and Innovation Centre, Fondazione Edmund Mach, San Michele all'Adige, Italy

^f Micalis Institute, INRAE, AgroParisTech Université Paris-Saclay, Jouy-en-Josas, France

^g Hydrosiences Montpellier, Institut de Recherche pour le Développement, CNRS, University of Montpellier, Montpellier, France

ARTICLE INFO

Editor: Marti Nadal

Keywords:

Transcriptome
 Arsenic
 Gene expression
 Blood
 Drinking water
 Bolivia

ABSTRACT

Chronic exposure to inorganic arsenic (As) in drinking water is a serious health concern but people differ in susceptibility. Naturally occurring As in Bolivian drinking water was recently reported, however, its long-term effects on the blood transcriptome remain unexplored. To bridge this gap, we conducted a transcriptome-wide analysis of whole blood cells from individuals in the Bolivian Andes. Blood and urine samples were collected for transcriptomic analysis, genotyping of *AS3MT* polymorphisms, and measurements of inorganic As metabolites in urine. Linear regression models were employed for extracting As-associated genes, and cell deconvolution to estimate cell fractions from the transcriptome. Functional annotations of the As-associated genes were performed using Ingenuity Pathway Analysis (IPA) and ClusterProfiler. Protein-protein interaction analysis was conducted to identify networks between As-associated genes. A total of 588 genes were identified from linear regression analysis and associated with downregulation of autophagy-related functions and a reduction in activated NK cells. Stratification by gender showed a significant enrichment of pathways related to carcinogenesis, oxidative stress, glucose metabolism, and epigenetic regulation in females, e.g., PI3K/AKT/MTOR signaling, HIF-1 signaling, insulin receptor signaling, and microRNA biogenesis pathway. Carriers of the *AS3MT* genotypes associated with a poorer As metabolism showed enrichment in DNA replication and cell proliferation, whereas carriers of the genotype associated with an efficient As metabolism showed suppression of autophagy and DNA damage pathways. Our data indicate the importance of the autophagy pathway in relation to As exposure, and its crosstalk with PI3K/AKT/mTOR and miRNA biogenesis, providing new insights into the biological pathway under As exposure. Overall, this study identified novel genome-wide changes in blood mRNA in response to long-term As exposure in Bolivia, an underrepresented population, laying groundwork for further study.

1. Introduction

Inorganic arsenic (As) is a widely distributed groundwater pollutant. Currently, it is estimated that between 94 million to 220 million people worldwide are exposed to As in drinking water in concentrations above the limit of 10 µg/L as recommended by WHO (Podgorski and Berg,

2020). Chronic As exposure can cause multiple and severe morbidities, such as cancers, skin and respiratory diseases, chronic kidney disease, and cardiovascular diseases (Abolli et al., 2024; Chain et al., 2024; Moon et al., 2012; Tang et al., 2023; Tchounwou et al., 2023). Arsenic is metabolised in the human body to methylarsonic acid (MMA), and dimethylarsinic acid (DMA) (Vahter, 1999) and a higher degree of As

* Corresponding author.

E-mail address: harri.alenius@ki.se (H. Alenius).

¹ Shared authorship.

<https://doi.org/10.1016/j.envint.2025.109727>

Received 24 April 2025; Received in revised form 30 July 2025; Accepted 11 August 2025

Available online 12 August 2025

0160-4120/© 2025 The Authors. Published by Elsevier Ltd. This is an open access article under the CC BY license (<http://creativecommons.org/licenses/by/4.0/>).

dimethylation is associated with less toxicity (De Loma et al., 2022a; Li et al., 2012; Pierce et al., 2012; Vahter, 1999). The As metabolism is influenced by genetic factors, particularly variation in the arsenic methylation transferase gene *AS3MT*, that determines the degree of As methylation (Engström et al., 2015), and in turn toxicity. Also gender is influential; men have in general a poorer methylation capacity than women (Lindberg et al., 2007). To date, As toxicity has been linked to multiple mechanisms of genotoxicity, including inhibition of DNA repair, telomere damage, oxidative stress (De Loma et al., 2022a; Li et al., 2012), and various types of epigenetic alterations (Ameer et al., 2017; Chain et al., 2024; Gao et al., 2015). Moreover, As was shown to be associated with biological functions related to insulin resistance, regulation of T-cells, apoptosis, and cell cycle pathways (Andrew et al., 2008; Rehman et al., 2020).

Although variations in gene expression in response to As exposure have been reported, most studies have used animal models or cell cultures (Kibriya et al., 2022; Kozul et al., 2009; Liu et al., 2024; Shukla et al., 2022). However, research on transcriptomic perturbations in long-term As-exposed humans using whole-transcriptome sequencing data, remains limited (Chen et al., 2020; Engström et al., 2017; Fry et al., 2007; Rehman et al., 2020). In previous studies, we reported elevated As levels in Bolivian drinking water and a high prevalence of genetic variants adapted to an efficient As dimethylation among humans living in the Bolivian Andes (De Loma et al., 2022b, 2019; Tirado et al., 2024). As transcriptomics has been shown to be of importance for hazard identification and health risk characterization (Cecchetto et al., 2023; Li et al., 2023; Sprenger et al., 2022), investigating gene expression variation and underlying biological functions associated with As exposure in Bolivians can provide evidence of gene expression targets associated with development of known As-related diseases (Rehman et al., 2020). However, information on As-exposed associated gene expression in Bolivians is to our knowledge non-existent.

In this study, we used whole-transcriptome RNA sequencing to investigate associations between As exposure and transcriptomic changes in the main indigenous communities in the Bolivian Altiplano, analyzing the full cohort as well as subcohorts stratified by gender and *AS3MT* genotype. This research enabled us to assess transcriptomic variation associated with As, alongside functional pathways. Our findings provide novel insights into transcriptomic changes and potential mechanisms which are relevant for risk assessment of As exposure, laying the groundwork for further studies.

2. Methods

2.1. Cohort description and sample collection

Men and women living in villages in the Bolivian Altiplano, with an approximate elevation of 3700 m above sea level, were recruited during four field trips between October 2021 and April 2023. Five villages are located in the southern part of Lake Poopó (Pampa Aullagas, Llapallapani, Santuario de Quillacas, Sevaruyo, and Santiago de Huari) and Chipaya, a village 120 km west of the lake, near Coipasa salt lake (Fig. S1). Villages were selected to provide a wide range of arsenic exposure based on the screening of As concentrations in drinking water performed within this geographic region in a previous study (De Loma et al., 2019).

The study group consisted of 227 men and women. Of these, 117 women and 47 men were identified as being of Aymara-Quechua ethnicity, while 41 women and 22 men as being of Uru ethnicity. The Aymara and Quechua ethnicities are the largest ethnic groups in the Bolivian Andes and relatively similar from a genetic perspective (Batai and Williams, 2014). Members of the Uru ethnicity reside more isolated in the Chipaya and Llapallapani villages, whereas the inhabitants of the four other villages belong to the Aymara-Quechua population. Study participants from these Aymara-Quechua groups were therefore considered as one study group. We assessed ethnicity based on reported

birthplace, complemented with information of the residency of the participant's parents and grandparents.

Participants were interviewed about their age, dietary habits, medical history, time of residence, smoking status, coca chewing, and alcohol consumption. In addition, height and weight were measured for the calculation of body mass index (BMI). The dietary questionnaire was designed for Bolivian populations living in the Altiplano and included questions about traditional Bolivian foods, covering staple foods, side dishes (such as meat and fish), fruits, and indigenous foods (e.g., chuño and coca). The intake of these food categories over the past month was recorded as binary.

Water, from multiple sources in each village, and spot urine samples were collected in 20 mL polyethylene bottles. Urine sticks (Combur-7 Test strips, Roche, Basel, Switzerland) were used to measure urinary pH, glucose, ketones, leucocytes, nitrites and protein immediately after sampling. Peripheral whole blood was collected in (1) Trace Elements NH Sodium Heparin tubes (Vacuette, Greiner Bio, Austria) for assessment of trace elements concentrations, in (2) EDTA tubes (Vacuette) for DNA extraction, and in (3) PAXgene Blood RNA Tubes (BD, Hombrechtikon, Switzerland) for RNA extraction. Hemoglobin measurements were performed in venous blood using HemoCue201+ (HemoCue, Ängelholm, Sweden) at the study sites.

Urine, water and blood samples were stored at -18°C during each field trip (generally three days long) in a portable freezer (ARB, Alice Springs, Australia). Samples were then transported to the Genetics Institute at Universidad Mayor de San Andrés (La Paz, Bolivia) and stored at -20°C until further shipment to Sweden. Samples were transported on dry ice to Karolinska Institutet (Stockholm, Sweden), where all further analyses took place within three months from collection.

The study was approved by the Swedish Ethical Authority (Ref: Nr 2021-02376) and the Bolivian Comité Nacional de Bioética (Ref: CNB-CEI-02/2021). Participants were given information providing details about the study, study objectives, and data collection protocols. Before registration, all participants signed the informed consent form, and for those under 18 ($n = 4$), their parents or guardians signed the consent form.

2.2. Trace elements determination in water, urine and blood

Trace element concentrations in water, urine and blood were measured by Agilent 7900 inductively coupled plasma-mass spectrometry (ICP-MS, Agilent Technologies, Santa Clara CA, USA) as described before (De Loma et al., 2020, 2019). The concentrations of As in water and urine were the focus for this study but we also included a few other elements, based on earlier findings of increased concentrations in the drinking water in this region (boron, and lithium) (De Loma et al., 2019) and earlier studies of toxic metals and interference with the transcriptome (lead and cadmium) (Bakshi et al., 2008; Jiang et al., 2017; Yamada et al., 2009).

The concentration of total urinary As (UAs) was determined and compared to the sum of inorganic As (iAs) and its metabolite fractions, methylarsonic acid (MMA) and dimethylarsinic acid (DMA), using ICP-MS measurement. The sum of measured As metabolites was slightly lower than measured total arsenic (average sum-As/total-UAs = 92 %, $n = 226$). This difference indicates a low level of other urinary As compounds, such as arsenosugars or arsenolipids. MMA, DMA, and As (represents the sum of As (III) and As (V)), were separated and measured by anion exchange chromatography (Agilent 1260 Infinity II LC system, Agilent Technologies, USA) coupled to a 7700x ICP-MS (Agilent) as described (Stråvik et al., 2023). To assure oxidation of As (III) to As (V), the urine samples were incubated with 10 % hydrogen peroxide before As separation in the anion-exchange column Hamilton PRP-X110 (250 \times 4.1 mm). To account for variations in urine dilution, spot urine trace element concentrations were adjusted to the mean urinary osmolality of the total study group (727 mOsm/kg). Urinary osmolality was measured

by a digital cryoscopic osmometer (OSMOMAT 030, Gonotec, Berlin, Germany).

Urine concentrations of inorganic As and its metabolites is a more accurate exposure estimate of inorganic As since the individuals in the study may use several wells for water intake as well as be exposed to As from food. The cut-off for the low group of exposure was UAs < 50 µg/L (n = 81, median 28 µg/L; 5 %, 95 % CI 15, 49), based on the fact that concentrations of 5–50 µg/L are found in the urine of subjects with no intake of seafood arsenic or excessive exposure to inorganic arsenic in drinking water or in the working environment (Water, 1999). The medium group of exposure was defined as UAs 50–150 µg/L (n = 76, 86 µg/L; 54, 144) and high exposure as >150 µg/L (n = 69, 236 µg/L; 157, 461) to obtain fairly similar sized groups.

For evaluation of the analysis accuracy, commercial reference materials (water, urine, and blood) were included in the runs and analyzed together with the samples. The reference materials used were NIST water 1643f and urine 2669-I/II (NIST, Gaithersburg MD, USA), Seronorm urine lot 1011644-L1, 1403080-L1, 1403081-L2, 1706878-L2 and Seronorm blood lot 1702821-L1, 2011920-L1, 2011921-L2 (Sero AS, Billingstad, Norway). Since there was no boron value specified for the Seronorm blood samples, they were spiked with boron standard. The level of detection (LOD) for each measured element was determined as the average of measured blank samples plus three standard deviations.

2.3. Genotyping

DNA was extracted from whole blood samples using the QIAamp DNA Blood Mini Kit (Qiagen, Hilden, Germany). We selected two SNPs on chromosome 10 that have been associated with As metabolism efficiency, namely rs3740393 (G/C) and rs17115100 (G/T) close to the As methylating gene *AS3MT*, where the C allele rs3740393 and the T allele of rs17115100 have been associated with lower percentage of MMA and higher DMA in urine, and thus, a more efficient As metabolism (De Loma et al., 2022b; Engström et al., 2011). Genotyping was performed using allelic discrimination of rs17115100 and rs3740393 (Thermo Scientific assay IDs C_25597854_10 and C_25804287_10, respectively) with TaqMan real-time PCR. Reactions were analyzed on the LightCycler 480 II instrument (Roche, Switzerland). The following PCR conditions were applied: an initial denaturation step of 10 min at 95 °C, followed by 45 cycles of 15 s at 92 °C and 90 s at 60 °C. PCR amplifications were conducted in 384-well plates with a total reaction volume of 5 µL. Negative controls (without DNA) were included on each plate. For quality control of genotyping data, more than 10 % of samples were re-analyzed in a separate round of experiments with a 100 % agreement between duplicates. Data quality was assessed by evaluating Hardy-Weinberg equilibrium using the conventional Chi-Square test.

2.4. RNA extraction and gene expression analysis

A total of 191 available blood samples (randomly distributed between the villages) in PAXgene Blood RNA Tubes were prepared for RNA-Seq. Total RNA was purified using the RNeasy Mini Kit (Qiagen, Hilden, Germany) according to the manufacturer's instructions and then resuspended in RNase-free water. Messenger RNA (mRNA) was purified from total RNA using poly-T oligo-attached magnetic beads. After fragmentation, the first strand cDNA was synthesized using random hexamer primers followed by the second strand cDNA synthesis. The library was ready after end repair, A-tailing, adapter ligation, size selection, amplification, and purification. The library was checked with Qubit and real-time PCR for quantification and bioanalyzer (Agilent, USA) for size distribution detection. Then, the libraries were sequenced on an Illumina HiSeq platform (Illumina, USA), and 150 bp paired-end reads were generated.

2.5. Profiling of gene expression

Raw sequence reads were quality-trimmed and filtered to Remove (1) reads with adapter contamination; (2) reads containing more than 10 % of N, which stands for the unidentified base; (3) reads that constitute more than 50 % of low-quality nucleotides (base quality <5). After removing low-quality sequences, 41.7 ± 10 million clean reads were obtained for further analysis. The mRNA counts table was generated from the RNA sequencing data. A gene was filtered out when its count was less than 10 in more than half of the samples. The gene counts table was normalized based on variance stabilizing transformation for further analysis using DESeq2 R package (Love et al., 2014). Finally, the filtered and normalized dataset included 15,434 genes for further statistical analysis.

2.6. Characteristics and covariates of transcriptome variations

To screen for the potential covariates, we analyzed the contribution of host characteristics to transcriptome variation. Briefly, we collected individual characteristics based on interviews and measurements including: village, anthropometry, medication history, dietary habits, lifestyle, element concentrations in blood and urine, and self-reported diseases. The participants' characteristics were further classified into the following eight categories: geography (village), medication (usage of antibiotics or other drugs), dietary habits (consumption frequencies of food stuff), general metadata (age, gender, occupation, smoking status, alcohol consumption, farm ownership, genotype), arsenic (UAs concentration and fractions of As metabolites), anthropometry (height, weight, BMI), diseases (diabetes, cancer, cardiovascular, and other diseases), and element exposure (urine or blood element concentrations of boron, cadmium, lead and lithium). The contribution of individual characteristics on transcriptome variation was identified by calculating the association between categorical or continuous phenotypes and gene expression ordination with *envfit* function in the *vegan* R package (999 permutations; p values were adjusted with the Benjamini-Hochberg method for multiple hypothesis testing, and FDR < 0.05 were set as the threshold for a significant difference). This function performs *manova* and linear correlations for categorical and continuous variables, respectively. Host factors with an effect size >0.04 and FDR < 0.05 (lithium, lead, and coca) from this analysis were included as covariates in the regression model 2. The effect sizes of host factors were pooled into the broader predefined categories, estimated with the *bioenv* function in the same package (Clarke and Ainsworth, 1993), which selects the combination of host factors with the strongest correlation to transcriptome variation.

2.7. Genes associated with arsenic exposure

The normalized gene counts table was imported into R (v4.2.1). We then fitted two linear regression models to identify genes associated with the UAs, adjusting for variables (1) model 1: gender, age, and smoking status; (2) model 2: gender, age, smoking status, lithium, lead, and coca. Since there is a high correlation ($r_s = 0.76$, $p < 0.05$) between urinary lithium and boron levels, to minimize multicollinearity in the regression models and simplify interpretation, we retained only urinary lithium in model 2 (Fig. S2). We also conducted further analyses stratified by *AS3MT* genotype (rs3740393, CC: 129 SNP major, 62 GG/GC: SNP minor), and by gender (137 female, 54 male) to provide a more homogenous analysis to explore the gene expression associated with As exposure that may be blurred by the analysis using full cohort. P-values were adjusted with the Benjamini-Hochberg method for multiple hypothesis testing, and FDR < 0.05 were set as the threshold for a significant association (Li and Barber, 2019). Heatmaps were generated using the *heatmap* package (v1.0.12) (Kolde, 2018).

2.8. Pathway enrichment analysis

To understand the variation in gene expression from the functional aspect, functional annotation of the genes extracted from linear regression models was conducted using ClusterProfiler (v4.6.2) with the functions `enrichGo` and `enrichKEGG` (Yu et al., 2012), and the FDR for cutoff was set as 0.05. Additionally, we also conducted canonical pathway enrichment and Gene Ontology (GO) analysis using the ingenuity pathway analysis platform (IPA, Qiagen, CA).

2.9. Protein-protein interaction (PPI) network

PPI network analysis of genes associated with As exposure was performed on the STRING website (<https://www.string-db.org>, Version 11.5) (Szklarczyk et al., 2019), and networks with a PPI enrichment $p < 0.05$ were included for visualization. The network was visualized with Cytoscape software (v3.9.1) (Smoot et al., 2011). All other graph visualizations were conducted using `ggplot2`, `ggsci`, and `ggpubr` in R (v4.2.1).

2.10. Leukocyte deconvolution analysis

CIBERSORTx is an online analytical tool to estimate the abundances of subset cell types using gene expression data (Chen et al., 2018). LM22 (Félix Garza et al., 2019) gene signature matrix was used as a gene signature reference in this analysis, and LM22 includes 22 different immune cells isolated from peripheral blood. The gene expression matrix from the RNA-seq was used as input to estimate the cell fractions in all the subjects, and the estimations are based on 1000 permutations, the FDR of all the predicted cell fractions were < 0.05 .

2.11. Statistics

Wilcoxon test was used initially to assess differences in characteristics between ethnic groups. Spearman correlation tests were used for water element concentrations. Data matrices from transcriptomic profiles and metadata were imported into R (v4.2.1). Unless otherwise stated, analysis was performed using a Mann-Whitney test to compare two groups and Kruskal-Wallis test for more than two groups. For normally distributed data, analysis was performed using a Student's *t*-test to compare two groups, and one-way ANOVA for more than two groups; for non-normally distributed data, analysis was performed using a Mann-Whitney test to compare two groups and Kruskal-Wallis test for more than two groups. The principal component analysis (PCA) was done by the `fviz_pca_ind` function in the R package `factoextra` (v1.0.7) (Greenacre et al., 2022). Permutational multivariate analysis of variance (PERMANOVA, 999 permutations) was used to determine the association between blood transcripts and subject parameters. PERMANOVA was performed using the R package `Vegan` (v2.5.6) with the function "adonis2". Arsenic exposure was used as a continuous variable in the regression models and as a categorical variable in the heatmap and PCA. *P* values were adjusted with the Benjamini-Hochberg method for multiple hypothesis testing, and $FDR < 0.05$ was set as the threshold for a significant difference.

3. Results

3.1. Study population characteristics

The study outline is summarized in Fig. 1 and the characteristics of the participants are shown in Table 1. A total of 227 individuals was included in the study and peripheral blood samples sufficient for transcriptome analysis were available for 191 participants, including 137 females and 54 males. There were no significant differences in age, gender, smoking, or As exposure between the full cohort and the cohort for transcriptomic analysis. For AS3MT rs3740393, there were 129 major carriers (genotype CC) and 62 minor carriers (CG or GG). The

genotype distribution for the whole cohort is shown in Table 1. A very similar number of individuals were obtained stratifying for rs17115100 (130 major carriers and 61 minor carriers), since rs3740393 and rs17115100 were in almost complete linkage disequilibrium. The study participants had in general a healthy lifestyle with low level of alcohol consumption or smoking. The majority (91 %) of the study participants had normal blood pressure, as defined by the WHO (systolic pressure < 120 mmHg and diastolic pressure < 80 mmHg). Median hemoglobin levels were, as expected at this high altitude, high; above 15 g/dL for both men and women. Few study participants reported disease: six participants (3 % of the study group) reported heart problems and/or infectious diseases, 13 participants (6 %) reported hypertension and 13 participants (6 %) reported diabetes, and one person (0.5 %) reported hypothyroidism. No individuals reported having cancer, goiter, or hyperthyroidism. Total urinary As concentrations (UAs) showed a wide range (11.1–504.4 $\mu\text{g/L}$; median: 72.1 $\mu\text{g/L}$ in men, 76.8 $\mu\text{g/L}$ in women), as well as within the villages (Table 1 and 2).

3.2. Trace elements in water, urine and blood

The As concentrations in water varied between the villages, ranging from 8.3 to 276.0 $\mu\text{g/L}$ (Table 2), but there was not a strong correlation between UAs and WAs as seen previously in this area (De Loma et al., 2019). The boron concentrations in water ranged from 310.1 to 4670.3 $\mu\text{g/L}$, and the lithium concentrations varied between 33.9 and 1099.1 $\mu\text{g/L}$. All water wells exceeded the current guidance value of 300 $\mu\text{g/L}$ for boron (Ministerio de Medio Ambiente y Agua and Viceministerio de Agua Potable y Saneamiento Básico, 2018). There is no guidance value for lithium in drinking water in Bolivia. We found moderate positive correlation between As and lithium concentrations in water ($r_s = 0.56$, $p = 0.00019$), and with boron concentrations in water ($r_s = 0.63$, $p = 1.9 \times 10^{-5}$). UAs showed a wide range (11.1–504.4 $\mu\text{g/L}$; median: 72.1 $\mu\text{g/L}$ in men, 76.8 $\mu\text{g/L}$ in women) (Table 1). The concentration of As in blood differed between the Aymara-Quechua and Uru groups, with median values of 2.0 $\mu\text{g/L}$ and 6.1 $\mu\text{g/L}$, respectively. The median blood concentration of lead was 16.7 $\mu\text{g/L}$, with no significant differences between ethnic groups.

3.3. Host factors associated with blood transcriptome variation

Metadata variables, i.e. host factors, of the study participants ($N = 40$) were analyzed in relation to variation in the transcriptome to identify the potential covariates to be adjusted in the regression model 2. A total of 12 variables were found to correlate significantly ($FDR < 0.2$) with overall transcriptome variation (Fig. 2A). Among these, geography, urine lithium concentrations, and UAs were the top three variables explaining blood transcriptome variation, followed by frequency of coca chewing, blood lead concentration, and gender, with decreasing effect sizes. UAs showed a significant effect on blood transcriptome variation (effect size $R^2 = 4.7$ %; $FDR < 0.05$). Moreover, factors with an effect size > 0.04 and $FDR < 0.05$ (the urine lithium concentration, frequency of coca chewing, and blood lead concentration) were adjusted in regression model 2. All metadata variables were then grouped into eight predefined categories (geography, medication, dietary habits, general metadata, As, anthropometrics, disease, and element exposure) and the combined effect size was assessed for each category. The element exposure category explained most of the blood transcriptome composition, accounting for 5.7 % of transcriptome variation (Fig. 2B). Diseases, geography, general metadata, dietary habits, and As followed with decreasing effect size on transcriptome variation.

3.4. Blood transcriptome associations with as exposure in Bolivians

After data filtering, a total of 15,434 genes were retained for further analysis. To assess variation in the transcriptome across different UAs exposure levels, the 191 participants were divided into three groups

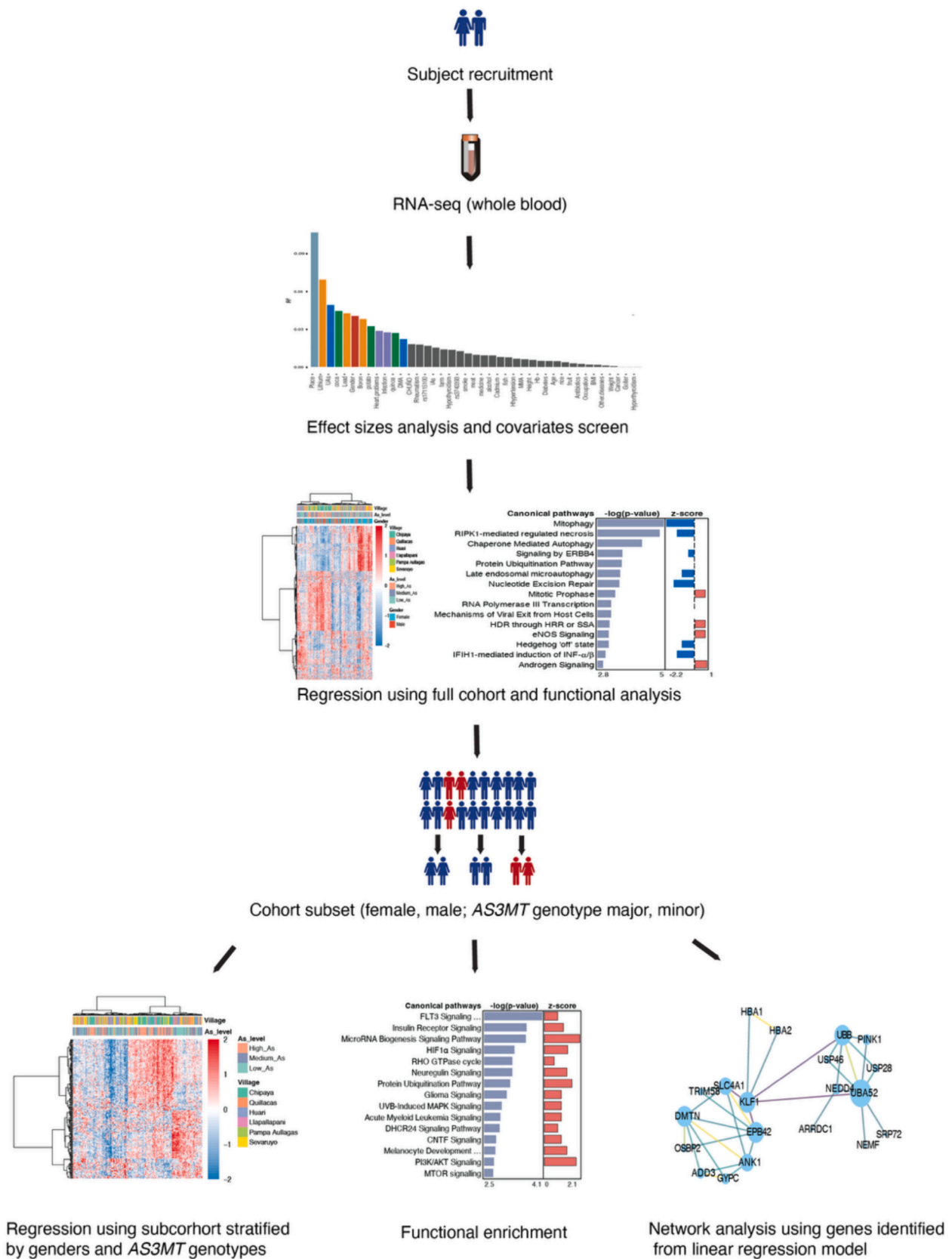


Fig. 1. Study outline. The graph summarizes the study design and analytical strategy. Human blood and urine samples were collected from individuals in the Bolivian Andes around Lake Poopó and Coipasa salt lake for RNA-seq and urine arsenic assessment, respectively. The effect size of host factors on gene expression was evaluated for identification of potential covariates. The linear regression model was fitted to identify arsenic-associated genes using the whole cohort and then stratified by *AS3MT* SNP genotypes (rs3740393 CC = major and CG and GG = minor) and gender.

Table 1
Characteristics of the study participants (total study group and stratified by ethnicity and sex). Data are presented as median (min–max) or percentage (%).

Characteristic	Total population		Aymara-Quechua		Uru		p-value ^a	
	n		n		n		Men	Women
Number of participants	n = 227		n = 164		n = 63			
Gender	Men, n = 69	Women, n = 158	Men, n = 47	Women, n = 117	Men, n = 22	Women, n = 41		
Age	50 (13–87)	41 (15–78)	50 (13–87)	46 (15–78)	50 (24–75)	34 (15–68)	0.842	<0.001
Height (cm)	162 (142–182)	152 (138–180)	162 (142–182)	152 (138–164)	161 (151–170)	151 (140–180)	0.264	0.399
Weight (kg)	68 (51–127)	65.5 (36–102)	69 (51–127)	66 (36–102)	68 (51–92)	62.5 (45–86)	0.274	0.178
Body mass index (kg/m ²)	27 (19–46)	28 (17–47)	27 (19–46)	28 (17–47)	26 (20–36)	28 (19–37)	0.331	0.404
Tobacco smoking (yes, %)	8.7	3.8	10.6	4.3	4.5	2.4	0.402	0.597
Alcohol (yes, %)	63.8	36.7	68.1	44.4	54.5	14.6	0.276	<0.001
Coca leaves (yes, %)	86.9	77.2	85.1	77.8	90.9	75.6	0.505	0.688
Blood pressure, systolic	120 (85–177)	110 (79–196)	120 (85–152)	111 (79–196)	119 (87–177)	106 (83–192)	0.357	0.065
Blood pressure, diastolic	75 (40–99)	72 (52–111)	75 (40–93)	73 (54–111)	80 (55–99)	70 (52–87)	0.154	0.016
Hemoglobin (g/dL)	17.6 (12.5–25.1)	15.5 (9.1–20.0)	17.7 (12.9–25.1)	15.8 (9.1–20.0)	17.0 (12.5–21.5)	15.1 (10.3–17.5)	0.261	0.016
Antibiotics (yes, %)	17.4	17.1	21.3	21.4	9.1	4.9	0.213	0.016
Total urinary As (µg/L) ^b	72.1 (17.1–445.3)	76.8 (11.1–504.4)	48.0 (17.1–318.7)	56.3 (11.1–297.4)	239.6 (87.6–445.3)	215.9 (22.5–504.4)	<0.001	<0.001
Blood As (µg/L) ^b	3.4 (0.7–15.4)	2.4 (0.5–22.1)	2.2 (0.7–7.2)	1.9 (0.5–7.6)	5.7 (2.4–15.4)	6.4 (1.1–22.1)	<0.001	<0.001
Urinary Cd (µg/L) ^b	0.3 (<LOD ^c -1.9)	0.5 (<LOD ^c -4.4)	0.3 (<LOD ^c -1.9)	0.5 (<LOD ^c -4.4)	0.5 (0.1–1.1)	0.5 (0.1–3.0)	0.067	0.760
Urinary B (µg/L) ^b	4457.0 (1375.3–20522.2)	5121.2 (851.0–28195.8)	3885.5 (1853.3–13128.9)	4448.9 (851.0–28195.8)	5964.0 (3229.3–20522.2)	9008.4 (1915.7–20347.7)	<0.001	<0.001
Urinary Li (µg/L) ^b	1309.7 (267.5–5057.5)	1170.5 (175.2–4857.5)	931.9 (267.5–5057.5)	1011.7 (175.2–4857.5)	1615.7 (811.9–2875.0)	1434.27 (242.6–3255.2)	<0.001	0.005
Blood Pb (µg/L)	19.1 (7.0–119.8)	14.9 (3.8–71.7)	18.9 (7.0–56.3)	16.1 (3.8–71.7)	20.6 (11.6–119.8)	13.7 (7.3–46.1)	0.847	0.293
AS3MT rs3740393 (%)								
CC	66.8		58.1		89.8		<0.001	
GC	26.2		32.9		8.5		<0.001	
GG	7		9		1.7		0.012	

^a p-Value for Wilcoxon rank-sum (Mann-Whitney) test when comparing medians and for z-test when comparing proportions.

^b Urinary concentrations of trace elements adjusted to average urinary osmolality (727 mOsm/kg).

^c The concentration of Cd in urine was below detection limit (LOD < 0.02 µg/L).

Table 2
Trace elements concentrations in urine and water from individuals and six villages in the Bolivian Altiplano.

Village	Urine		Water ^b					
	n	Arsenic (µg/L) ^a	n	Arsenic (µg/L)	Boron (µg/L)	Lithium (µg/L)	Cadmium (µg/L)	Lead (µg/L)
Chipaya	53	244.7 (22.5–504.4)	2	276; 212	4670; 2844	627; 742	0.06; 0.19	0.03; 0.23
Llapallapani	3	96.9 (39.3–106.9)	1	26	310	40	<LOD ^c	1.33
Pampa Aullagas	16	33.7 (14.5–96.1)	1	26	717	102	<LOD ^c	2.43
Santuario de Quillacas	40	52.5 (13.0–268.7)	3	92; 31; 70	3119; 2172; 1341	810; 552; 105	<LOD ^c ; <LOD ^c ; <LOD ^c	0.76; 0.32; 2.37
Sevaruyo	35	136.4 (21.5–318.7)	4	93; 108; 57; 8	2455; 3345; 1226; 1516	914; 1099; 75; 108	<LOD ^c ; <LOD ^c ; <LOD ^c ; <LOD ^c	0.35; 0.11; 0.38; 2.09
Santiago de Huari	44	38.7 (11.1–119.3)	3	15; 15; 14	1048; 846; 756	39; 35; 34	0.03; 0.05; <LOD ^c	0.23; 0.24; 0.08

^a Total As concentration in urine (adjusted to average urinary osmolality) presented as median (minimum–maximum).

^b Results for water are presented as concentration for each individual water source.

^c The concentration of Cd in water was below detection limit (LOD < 0.02 µg/L).

based on total urinary As concentrations: low (< 50 µg/L, median UAs 28 µg/L; 5 %, 95 % CI 15, 49), medium (50–150 µg/L, 84 µg/L; 54, 143), and high (>150 µg/L, 253 µg/L; 160, 467). We performed principal component analysis (PCA) on the blood transcripts (Fig. 3A, Supplementary Table 1). PCA of blood transcripts showed no significant difference between As exposure groups (FDR = 0.36). We then fitted the linear regression model 1 to identify genes associated with UAs. A total of 588 genes correlated with As exposure (FDR < 0.05), with 226 genes positively associated with UAs and 362 negatively associated.

Unsupervised hierarchical clustering analysis of these genes revealed distinct sub-clusters among different subsets of samples (Fig. 3B).

The top three genes that correlated with UAs after FDR correction were *CHORDC1* (+; i.e. higher gene expression with higher UAs), *PLVAP* (–), and *ISL2* (–) (Fig. 4A). Genes that exhibited significant correlations were subsequently annotated based on canonical pathways and molecular functions using IPA. Functions related to carcinogenesis, such as autophagy, necrosis, and mitophagy, were identified as down-regulated, and the Endothelial nitric oxide synthase (eNOS) signaling pathway and

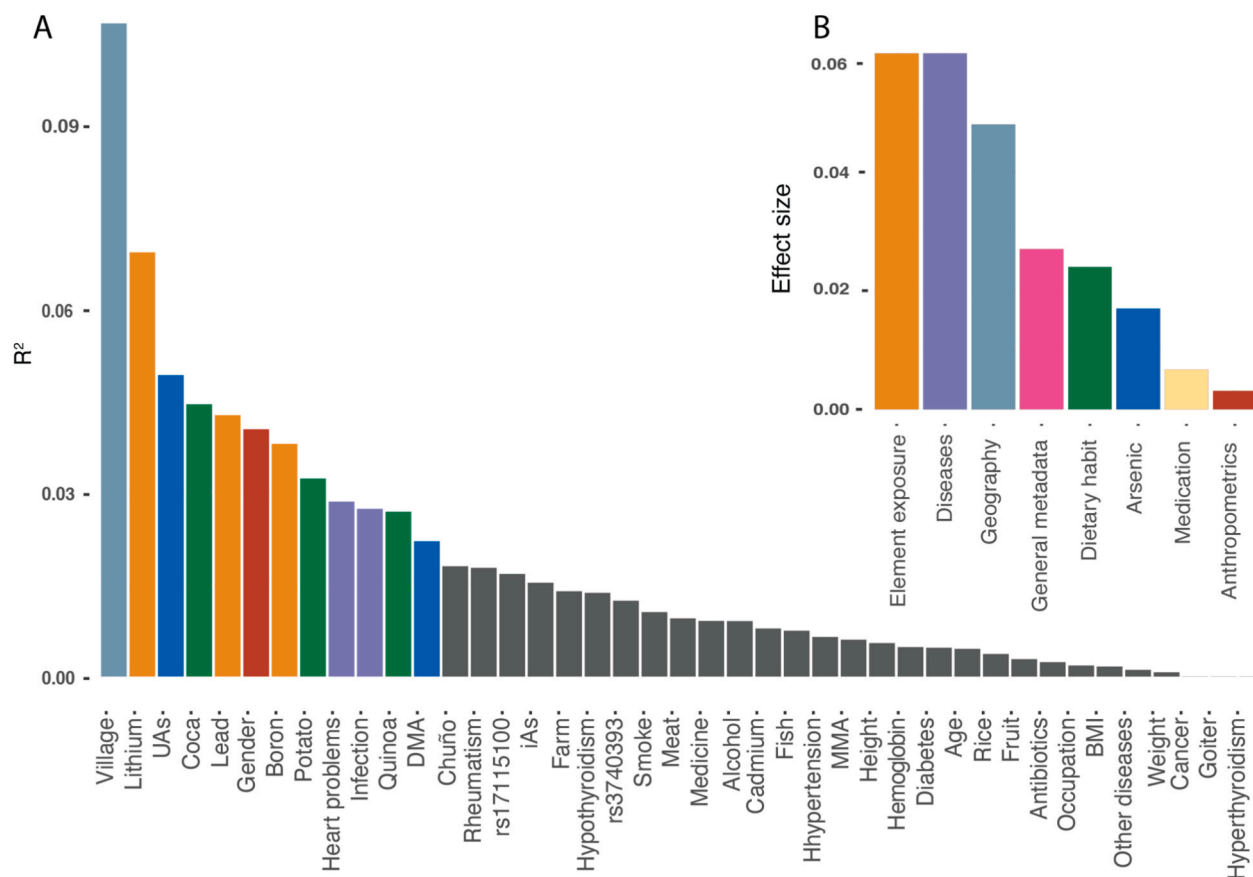


Fig. 2. Contribution of host factors in blood transcriptome variation and their effect sizes. A. The effect size of metadata variables on the variation of the blood transcriptome. The contribution of individual characteristics on transcriptome variation was identified by calculating the association between categorical or continuous phenotypes and gene expression ordination via envfit (vegan) and those with statistical significance ($FDR < 0.2$) were colored based on the metadata categories in Fig. 2B. B. Combined effect size of host factors were pooled in predefined categories with covariate distance-based selection: Element exposure (urine and blood element concentrations of boron, cadmium, lead, lithium), Diseases (diabetes, cancer, heart, and other diseases), Geography (village), General metadata (age, gender, occupation, smoking status, alcohol consumption, farm ownership, genotype), Dietary habit (consumption frequencies of food stuff), Arsenic (UAs concentrations and metabolite fractions), Medication (usage of antibiotics or other drugs), and Anthropometrics (height, weight, BMI). Lithium: urine lithium concentration, Boron: urine boron concentration, Cadmium: urine cadmium concentration, iAs: urine inorganic arsenic concentration, UAs: total urine arsenic, Lead: blood lead concentration.

erythroid-related functions were up-regulated with higher As exposure (Fig. 3C, D). Autophagy-associated functions were enriched through GO term annotation using clusterProfiler as well. Additionally, the AMPK signaling pathway and longevity pathways were identified through KEGG annotation (Fig. S3A, B). To better understand interactions among genes associated with UAs, we constructed a protein–protein interaction (PPI) network. Subnetworks related to autophagy (HSP90AA1-centered) and tumorigenesis emerged from the PPI analysis (Fig. 4B). Since peripheral blood mononuclear cells reflect immune system cells, we applied CIBERSORT deconvolution analysis using LM22, a reference signature matrix encompassing major lymphocyte types. Interestingly, the predicted levels of activated NK cells were significantly lower in the high As exposure group compared to medium and low exposure groups at the $FDR < 0.2$ (Fig. 4C).

In model 2. The number of blood transcripts associated with UAs was reduced to 358 genes, however, there were still clear patterns among different subsets of samples (Fig. S4A). The top 10 GO and KEGG annotation terms were also related to autophagy, red blood cell development, and AMPK signaling pathway (Fig. S4C, D). The PPI analysis showed three subnetworks related to ubiquitin, erythrocyte membrane, and MAPK, respectively (Fig. S4B).

3.5. Arsenic associated genes in females and males, respectively

Since the full cohort consists of subjects of different genders, which may dilute the signal of genes associated with As exposure, to provide a more homogenous analysis to explore the gene expression associated with As exposure from different aspects, subsequent analysis was performed on the data stratified by gender. There were 225 genes related to UAs in females, and among those, 168 genes overlapped with the results based on the whole cohort and 57 were unique, however, there were no genes associated with UAs in males at the $FDR < 0.05$ (Fig. 5A, B). Functional annotation on As-associated genes in females, identified the pathway related to carcinogenesis, diabetes, and epigenetics, such as the PI3K/AKT/MTOR, HIF-1 signaling pathways, insulin receptor pathway, and microRNA biogenesis pathway. In terms of molecular functions, cell cycle-related terms were enriched (Fig. 5C, D). PPI analysis revealed a network centered on HSP90AA1 and AKT associated with autophagy (Fig. 5E).

In model 2, consistent with our findings, only one As-related gene was identified in males, while in females, UAs-related genes declined to 76. Of these, 58 overlapped with As-associated genes identified in the whole cohort, and 18 were unique (Fig. S5A). Unsupervised hierarchical clustering analysis revealed similar patterns as model 1 (Fig. S5B), with KEGG annotation highlighting enrichment in the EGFR tyrosine kinase inhibitor resistance and HIF-1 signaling pathways (Fig. S5C).

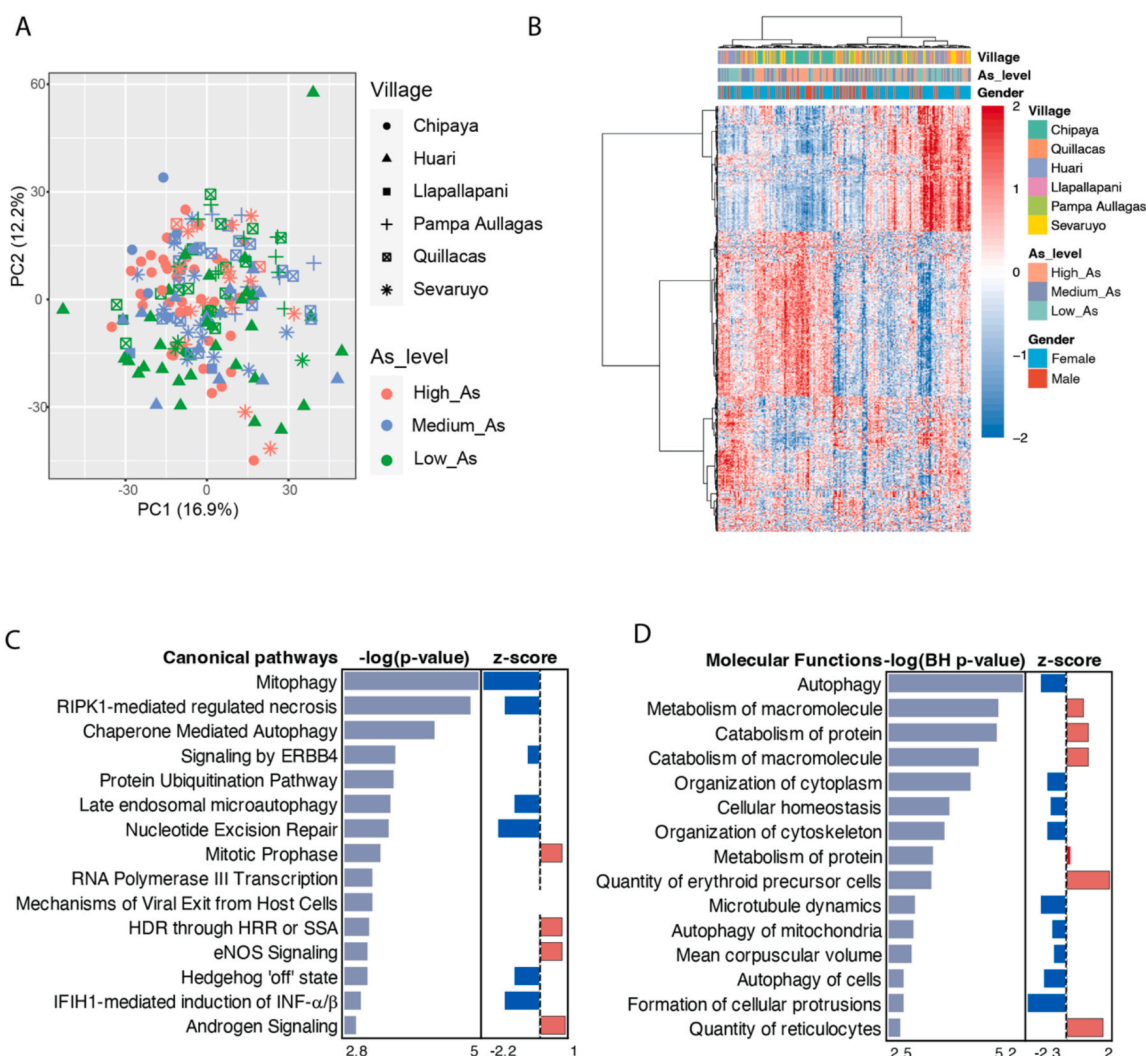


Fig. 3. Host genes correlated with arsenic (As) exposure among all village people. (A) The host transcriptome was analyzed and plotted via principal component analysis (PCA) based upon the Bray-Curtis dissimilarities with village (shape) and As exposure level in urine (as the sum of arsenic metabolites) categorized in three groups, high, medium, and low (color). (B) Heatmaps summarize host genes associated with As exposure. Host genes correlating with the As exposure were further annotated based on canonical pathways (C) and molecular functions (D) using IPA. This association was assessed using linear regression model adjusted for gender, age, and smoke status (FDR < 0.05).

3.6. Arsenic associated genes in AS3MT major and minor, respectively

In addition to the gender-stratified analysis, we fitted a regression model on data stratified by *AS3MT* genotype, i.e. rs3740393 CC carriers (major, associated with a more efficient As metabolism) and CG and GG (minor, associated with a less efficient As metabolism) carriers. In the major group, we identified 235 UAs-related genes, 173 of which overlapped with As-associated genes from the full cohort, while 62 were unique. In the minor allele group, 30 As-related genes were found, with 5 overlapping genes from the full cohort and 25 unique (Fig. 6A). Unsupervised hierarchical clustering analysis revealed two sub-clusters within each *AS3MT* group. In rs3740393 major, one cluster was associated with high As exposure (Fig. 6B), while in SNP minor, a cluster correlated with low and medium As exposure was identified (Fig. 6C). IPA analysis predicted the suppression of autophagy and DNA damage pathways in rs3740393 major carriers, while minor carriers showed enrichment in DNA replication and cell proliferation terms (Fig. 6D, E). As-associated genes were also used to construct PPI networks for rs3740393 major and minor groups (Fig. 6F, G). In rs3740393 major, predicted interactions included a ubiquitin-related sub-network.

In model 2, rs3740393 major, the number of UAs-related genes was

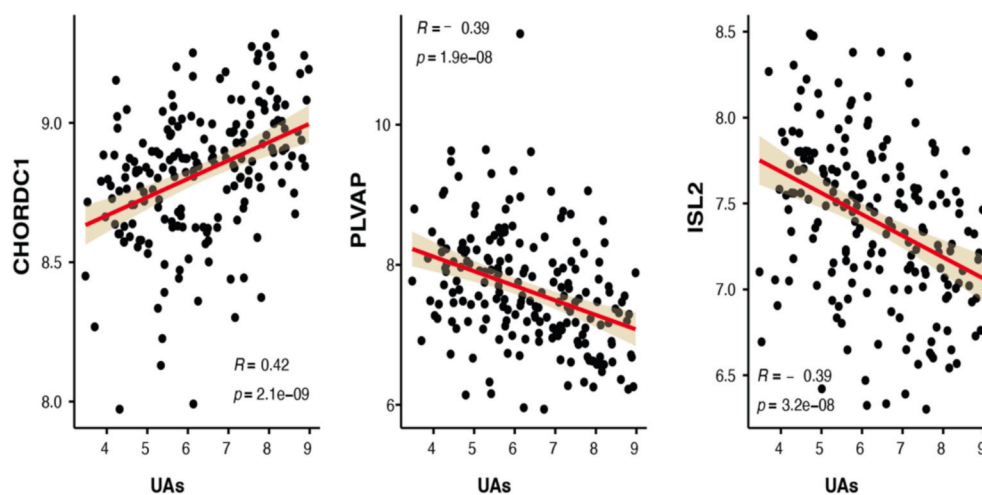
reduced to 139, of which 121 overlapped with As-associated genes identified from all samples, while 18 were unique. In rs3740393 minor, the number of UAs-related genes declined to 5 (Fig. S6A). Unsupervised hierarchical clustering analysis revealed two sub-clusters (Fig. S6B), with GO term enrichment highlighting functions related to erythrocyte and myeloid cell development, as well as a Parkinson's disease-related pathway (Fig. S6C, D; Fig. S7).

Finally, we stratified by gender within the *AS3MT* major subgroup (Fig. S8). There was no gene associated with As in males. In females within the major genotype subgroup, there are similar clustering patterns to the analysis based on all females, which indicates that the As-related gene expression among women still exists within *AS3MT* major genotype subgroup.

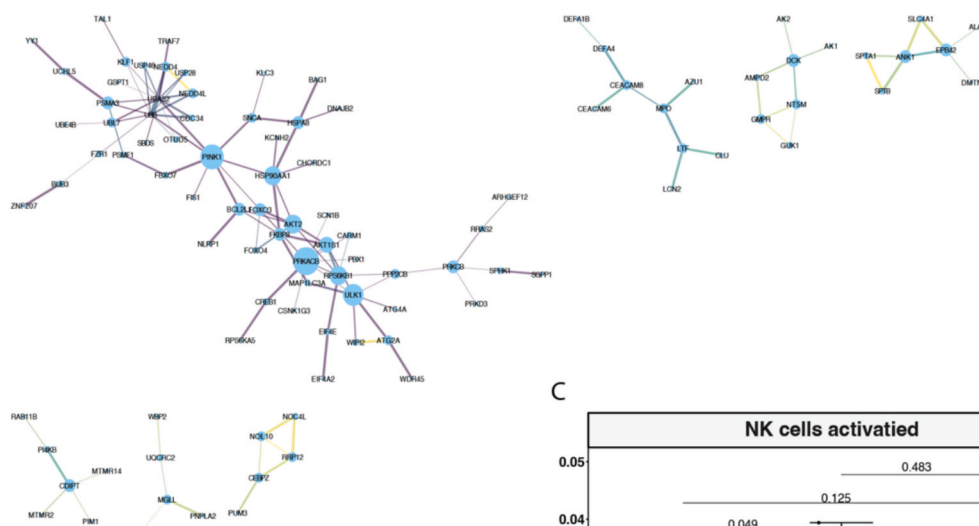
4. Discussion

This study is based on the three major indigenous groups living in the Bolivian highlands, and area with naturally elevated As concentrations in drinking water (De Loma et al., 2019). Despite the As exposure, the study participants reported few health problems and had in general normal blood pressure. This may partly be related to the fact that the

A



B



C

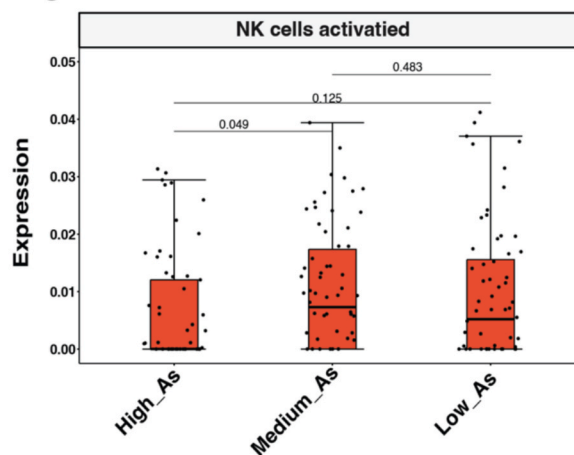


Fig. 4. Protein-protein interaction and leukocyte composition analysis of host genes correlated with arsenic (As) exposure among all village people. (A) The Spearman correlation between total urine As concentration (UAs) with the top three host genes derived from the regression analysis. The grey shadow refers to the 95 % confidence interval. (B) Host genes that correlated with As exposure were further examined for Protein-Protein Interaction (PPI) networks using the STRING database (V11.5) and visualized with Cytoscape. The node size is proportional to the degree of its connectivity to other nodes. All PPI networks exhibited an enrichment value of $p < 1 \times 10^{-10}$. (C) Boxplots depict differences in immune cell expression deconvoluted via the Cibersort (CS) algorithm. High_As: high level of As exposure; Medium_As: medium level of As exposure; Low_As: low level of As exposure; Within each boxplot, horizontal lines denote median values; boxes extend from the 25th to the 75th percentile of each group's distribution of values.

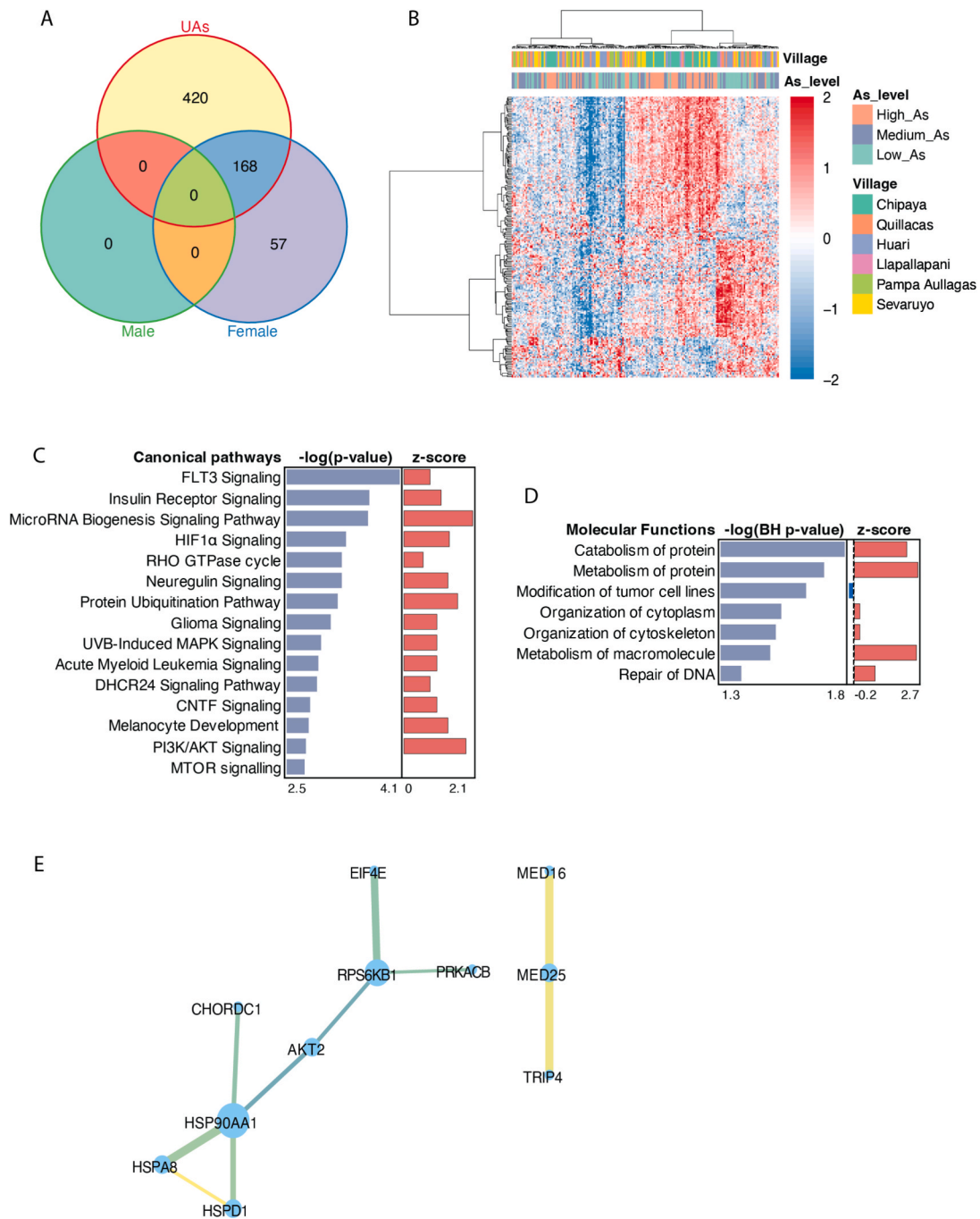


Fig. 5. Host genes correlated with arsenic (As) exposure in female Bolivians. (A) Venn plot showed the number of overlapping and distinct As-associated genes based on all the Bolivians, females, and males. (B) Heatmaps summarize host genes associated with As exposure. Host genes correlating with the As exposure were further annotated based on canonical pathways (C) and molecular functions (D) using IPA. (E) Host genes that correlated with As exposure were further examined for Protein-Protein Interaction (PPI) networks using the STRING database (V11.5) and visualized with Cytoscape. The node size is proportional to the degree of connectivity to other nodes. All PPI networks exhibited an enrichment value of $p < 1 \times 10^{-10}$. This association was assessed using linear regression model adjusted for age and smoke status (FDR < 0.05).

inhabitants in this area carry a very high allele frequency *AS3MT* genotypes associated with an efficient As metabolism, limiting some adverse effects of As. However, when taking multiple individual characteristics, including genetics and co-exposures, into account, As still explained a significant part of the blood transcriptome variation. Further, downstream analysis stratifying the cohort by gender and *AS3MT* genotype provides a more homogeneous analysis. Our findings highlight the complex relationship between the blood transcriptome and long-term As exposure, as well as the underlying autophagy, PI3K/AKT/

MTOR, and microRNA biogenesis pathway linked to As-associated health implications, laying the groundwork for understanding host transcriptome variation under chronic As exposure in different population groups.

When applying model 1, 588 As-associated genes were identified and linked to various biological processes, of which *CHORDC1*, *PLVAP*, and *ISL2* were the top three associated genes. More arsenic was reported to be associated with higher expression of the *CHORDC1* gene and higher abundance of Morgana, a co-chaperone protein of HSP90 coded by the

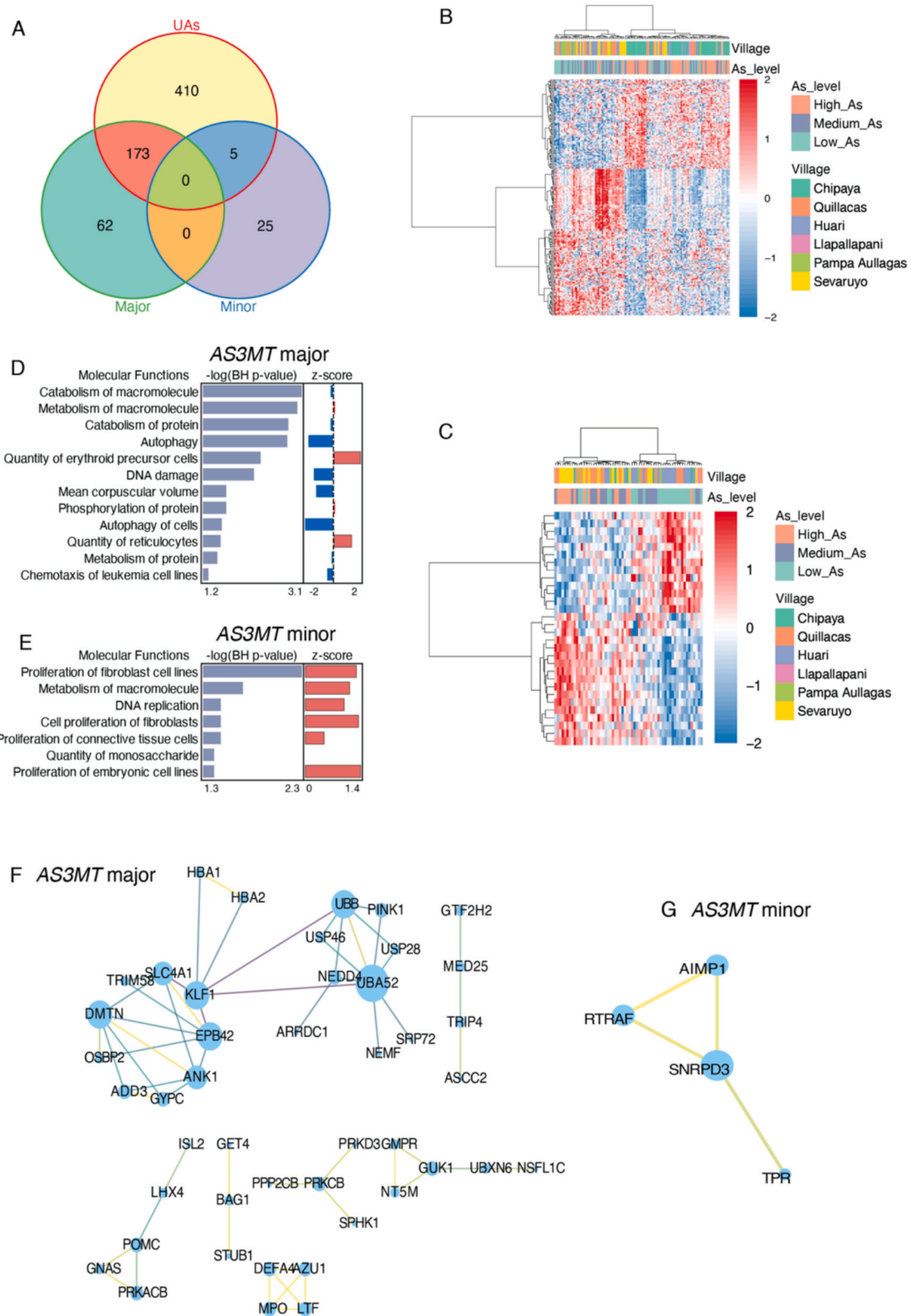


Fig. 6. Genes correlated with arsenic (As) exposure in *AS3MT* majors (rs3740393 CC) and minors (CG and GG) respectively. (A) Venn plot showed the number of overlapping and distinct As-associated genes based on all the Bolivians, *AS3MT* (rs3740393) major genotype (CC), and *AS3MT* minors (CG + GG). Heatmaps summarize host genes associated with As exposure in SNP majors individuals (B) and in SNP minors individuals (C). Genes correlating with the As exposure were further annotated for SNP majors (D) and SNP minors (E) using IPA. Genes that correlated with As exposure were further examined for Protein-Protein Interaction (PPI) networks for SNP majors (F) and SNP minors (G) using the STRING database (V11.5) and visualized with Cytoscape. The node size is proportional to the degree of its connectivity to other nodes. All PPI networks exhibited an enrichment value of $p < 1 \times 10^{-10}$. This association was assessed using linear regression model adjusted for gender, age, and smoke status (FDR < 0.05).

CHORDC1 (Freedman et al., 2025; Fusella et al., 2017; Xie et al., 2020). Overexpression of *CHORDC1* and subsequent Morgana may lead to the activation of NF- κ B, involved in regulating autophagy, and consequently, the onset of various types of cancers (Fusella et al., 2017; Poggio et al., 2024). Similarly, the expression of *ISL2* and *PLVAP* was found to be related to carcinogenesis in other studies (Ozturk et al., 2022; Ferreccio et al., 2013; Liu and Liu, 2024; Zhang et al., 2021), and these genes need further validation for As-related carcinogenesis.

Carcinogenesis is one of the major adverse outcomes of exposure to As, and autophagy plays a key role in the onset/development of tumors (Debnath et al., 2023). Cell models showed that As exposure could disturb autophagy (Wu et al., 2020). Our functional annotation of As-associated genes in the blood transcriptome suggests that As exposure may influence oxidative stress and autophagy associated pathways, including the PI3K/AKT/mTOR signaling pathway and AMPK that have been found to play a role in autophagy induction or inhibition with metal exposure (Chen and Costa, 2018). AKT activation, which is upregulated in many tumors, leads to mTOR activation and blockage of autophagy, and there is evidence that defects in autophagic responses are associated with carcinogenesis (Peng et al., 2022; Apel et al., 2009). Based on previous studies showing that various carcinogenesis-associated pathways are enriched in response to arsenic exposure (Rehman et al., 2020; Chen et al., 2020), our findings suggest that the autophagy pathway may play a key role in arsenic-associated carcinogenesis. However, no one in our cohort reported cancer, and earlier research shows that the Uru and Aymara/Quechua people living in this area have developed a genetic adaptation to arsenic (De Loma et al., 2022b). This may indicate a more complicated mechanism due to the interaction of different omic layers, which needs further investigation. Molecular functions such as cellular homeostasis and organization of the cytoskeleton suggest a broader disruption of cellular stress responses and metabolic dysregulation, consistent with prior reports of As-induced cytotoxicity and impaired cellular integrity (Xie et al., 2014). Additionally, necroptosis (RIPK1-mediated) and DNA damage-related pathways reflect apoptosis and mitochondrial dysfunction, which are key features of As-induced cytotoxicity and carcinogenesis (Yang et al., 2025). The protein ubiquitination pathway is strongly associated with oxidative stress and cellular dysfunction, which are well-established consequences of As exposure (Jiang and Wang, 2022; Tsou et al., 2005). The enrichment of RNA Polymerase III Transcription and IFI1-mediated induction of INF- α/β points to potential modulation of innate immune responses and associated inflammation, aligning with arsenic's known impact on inflammation (Reverendo et al., 2019). Our PPI analysis of the As-related genes revealed that proteins associated with autophagy (e.g., PINK1, HSP90AA1), cell cycle (e.g., ULK1, RPS6KB1), and erythrocyte membrane (e.g., EPB42) were interconnected, forming distinct sub-networks. Consistent with our findings, previous cell line studies have shown that As exposure may induce IL-6 overexpression and block autophagic flux, leading to dysregulated autophagy (Lau et al., 2013; Qi et al., 2014). Notably, cell deconvolution analysis indicated decreased levels of activated NK cells in the high As exposure group compared to medium and low exposure groups, suggesting that high As exposure may suppress the immune system, as seen in other studies (Ferrario et al., 2016). Studies indicate a dual role for NK cells under As exposure: they may initially protect against tumor onset, but high As levels could impair NK cell function, allowing tumorigenic cells to evade immune surveillance (Boss et al., 2023; Sumi et al., 2021).

Gender is a well-known factor for susceptibility towards As exposure, partly due to the fact that women are more efficient in As metabolism than men (Muhetaer et al., 2022; Vahter et al., 2007). Regression analysis based on the full cohort, including both genders and *AS3MT* genotype, may blur the signal of genes associated with As exposure. To provide a more homogenous analysis, we conducted a subsequent analysis stratified by gender/genotypes. As-associated genes were identified in females but not in males, which may be due to the relatively lower sample size of males after stratification, or due to biological

differences in response to As exposure. We then performed IPA analysis to annotate the functions of these genes in females. Unlike the pathways identified in the full cohort, all pathways in females were upregulated. Several of the enriched canonical pathways in females, such as insulin receptor signaling, PI3K/AKT signaling, and mTOR signaling, are central regulators of cellular survival, and are known to be dysregulated under As exposure. Notably, PI3K/Akt/mTOR signaling pathway was found to cross-talk with autophagy and plays a role in promoting carcinogenesis under As exposure (Chen and Costa, 2018). Additionally, the enrichment of HIF1 α and MAPK signaling pathway indicates a response to oxidative stress and hypoxic conditions, both of which are activated by As exposure and induce the formation of cancer-like cells (Bi et al., 2020; Juan et al., 2023). Moreover, As has been shown to induce insulin resistance and alter glucose metabolism, and a study of As-related gene expression in blood showed the enrichment of insulin resistance pathway (Rehman et al., 2020). Long-term As exposure has in some studies been associated with an increased risk of developing type 2 diabetes (Chain et al., 2024). Our study showed the upregulation of insulin receptor signaling in females, suggesting a compensatory response to impaired insulin signaling, which may reflect inhibition of insulin-stimulated glucose metabolism and potentially contribute to insulin resistance under the As exposure. Six percent of the full cohort reported diabetes in the questionnaires, and a follow-up of our findings could be to evaluate genes of the insulin resistance pathway in diabetes cases and controls in As-enriched areas in Bolivia. Interestingly, the microRNA biogenesis pathways and glioma were enriched in females. Arsenic may induce epigenetic alterations, including miRNA dysregulation (Cardoso et al., 2018). Our findings suggest that As exposure may impact miRNA processing, and, in parallel with its known effects on DNA methylation, further disrupt the host gene expression. However, the mechanism of miRNA in carcinogenesis caused by As exposure remains unknown, but is worth further study. Together, these findings suggest a range of signaling and metabolic pathways that align with oxidative damage, metabolic regulation, and epigenetic regulation are involved in the As associated pathogenesis.

AS3MT is the main As methylating gene (Dheeman et al., 2014; Drobná et al., 2013; Torbøl Pedersen et al., 2020), and variation in this gene may cause differences in *AS3MT* expression under As exposure (Engström et al., 2011), differences in As metabolism (Engström et al., 2013). In *AS3MT* major subgroup, we observed strong enrichment in functions related to autophagy, DNA damage, and macromolecule catabolism, which are in line with established arsenic toxicological mechanisms, including oxidative stress, protein damage, and genotoxicity (Tam et al., 2020). These findings are consistent with our results using the full cohort, indicating that As carcinogenesis is associated with the imbalance of cellular function, especially the autophagy pathway, which plays an important role in As carcinogenesis. Additionally, in *AS3MT* minor subgroup, we observed significant enrichment in cell proliferation-related functions, particularly those involving fibroblasts and connective tissue cells. Several studies have been done to show that low levels of arsenic increased proliferation in keratinocytes and dermal fibroblasts (Germolec et al., 1996; Vega et al., 2001). Chien et al. found that chronic exposure to low levels of As increased cell growth and cell density in the HaCaT cell (Chien et al., 2004). This proliferation-enhancing effect is postulated to contribute to arsenic's ability to cause skin cancer (Trouba et al., 1999).

This study has some limitations. Our dataset is cross-sectional, which restricts our ability to investigate changes in gene expression over time under As exposure. Additionally, we used bulk RNA-seq data from peripheral blood cells rather than single-cell sequencing; while we were able to estimate cell fractions in blood samples, we could not isolate specific cell markers or variations within individual cell types related to As exposure. Moreover, since this is an exploratory study, further research is needed to clarify the mechanisms and interactions between genes and proteins, and the role of the ethnicity on the genes expression associated with As exposure. Despite these limitations, our study

provides a comprehensive profile of how long-term As exposure affects gene expression in the peripheral blood of Bolivians, offering valuable insights for future research.

In conclusion, our RNA-seq analysis has revealed variations in the blood transcriptome of Bolivians associated with long-term As exposure, notably the downregulation of autophagy pathways, which may be a key feature in the response to As in this population, and further study targeting the autophagy pathway is highly needed to understand its role in As-related disease. Additionally, our findings suggest that there might be a dose-dependent response to the As exposure, and high exposure may suppress the immune system. By stratifying genders and AS3MT genotypes, PI3K/AKT/mTOR and miRNA biogenesis associated pathways were enriched, indicating the crosstalk between autophagy with PI3K/AKT/mTOR in As carcinogenesis and the importance of exploring the effect of As exposure by integration of multi-omics data in future work. Overall, our results provide new insights into the relationship between host gene expression and long-term As exposure in Bolivian Andes, advancing our understanding of the mechanisms underlying As-induced diseases, and shedding light on further study in this area.

CRedit authorship contribution statement

Ying Yang: Writing – review & editing, Writing – original draft, Visualization, Formal analysis, Conceptualization. **Anastasiia Snigireva:** Writing – original draft, Project administration, Formal analysis. **Jessika Barron:** Writing – review & editing, Resources, Project administration. **Noemi Tirado:** Writing – original draft, Software, Conceptualization. **Maria Teresa Alvarez Aliaga:** Writing – original draft, Resources, Conceptualization. **Gina Torres:** Resources, Project administration. **Paolo Manghi:** Writing – review & editing. **Philippe Gérard:** Writing – review & editing. **Michael Levi:** Writing – review & editing, Formal analysis. **Jacques Gardon:** Writing – review & editing, Resources, Conceptualization. **Harri Alenius:** Writing – review & editing, Writing – original draft, Visualization, Formal analysis, Conceptualization. **Karin Broberg:** Writing – review & editing, Resources, Conceptualization.

Declaration of competing interest

The authors declare that they have no known competing financial interests or personal relationships that could have appeared to influence the work reported in this paper.

Acknowledgments

The authors warmly thank all study participants who participated in our study. We also thank Franz Ascuí Medical doctor from Oruro for his help during the field activities. We are grateful to everyone else who assisted during the recruitment, including workers at the local health centers, and to Marina Cuti at the Instituto de Genética.

This work was funded by the Institut de Recherche pour le Développement (France), the Hydrosociences Montpellier Laboratory (France), the Swedish Research Council (Sweden, DnR 2020-02827), Karolinska Institutet (Sweden), and the Genetics Institute at Universidad Mayor de San Andrés (Bolivia).

Appendix A. Supplementary data

Supplementary data to this article can be found online at <https://doi.org/10.1016/j.envint.2025.109727>.

Data availability

The data supporting the findings of this study are available from the authors upon reasonable request: transcriptomics data from [HA], and other data from [KB].

References

- Abolli, S., Dehghani, S., Atlasi, R., Maleki, Z., Yunesian, M., Tabatabaei-Malazy, O., Saraei, M., Khosravifar, M., Soleimani, Z., 2024. Arsenic and type 2 diabetes: revealing the environmental exposure relationship through effective factors - a systematic review. *Results Eng.* 22, 102054. <https://doi.org/10.1016/j.rineng.2024.102054>.
- Ameer, S.S., Engström, K., Hossain, M.B., Concha, G., Vahter, M., Broberg, K., 2017. Arsenic exposure from drinking water is associated with decreased gene expression and increased DNA methylation in peripheral blood. *Toxicol. Appl. Pharmacol.* 321, 57–66. <https://doi.org/10.1016/j.taap.2017.02.019>.
- Andrew, A.S., Jewell, D.A., Mason, R.A., Whitfield, M.L., Moore, J.H., Karagas, M.R., 2008. Drinking-water arsenic exposure modulates gene expression in human lymphocytes from a U.S. Population. *Environ. Health Perspect.* 116, 524. <https://doi.org/10.1289/ehp.10861>.
- Apel, A., Zentgraf, H., Büchler, M.W., Herr, I., 2009. Autophagy—a double-edged sword in oncology. *Int. J. Cancer* 125, 991–995. <https://doi.org/10.1002/ijc.24500>.
- Bakshi, S., Zhang, X., Godoy-Tundidor, S., Cheng, R.Y.S., Sartor, M.A., Medvedovic, M., Ho, S.-M., 2008. Transcriptome analyses in normal prostate epithelial cells exposed to low-dose cadmium: oncogenic and immunomodulations involving the action of tumor necrosis factor. *Environ. Health Perspect.* 116, 769–776. <https://doi.org/10.1289/ehp.11215>.
- Batai, K., Williams, S.R., 2014. Mitochondrial variation among the aymara and the signatures of population expansion in the central andes. *Am. J. Hum. Biol. Off. J. Hum. Biol. Counc.* 26, 321–330. <https://doi.org/10.1002/ajhb.22507>.
- Bi, Z., Zhang, Q., Fu, Y., Wadgaonkar, P., Zhang, W., Almutairy, B., Xu, L., Rice, M., Qiu, Y., Thakur, C., Chen, F., 2020. Nrf2 and HIF1 α converge to arsenic-induced metabolic reprogramming and the formation of the cancer stem-like cells. *Theranostics* 10, 4134. <https://doi.org/10.7150/thno.42903>.
- Boss, A.P., Freeborn, R., Jin, Y., Kaiser, L., Gardner, E., Rockwell, C.E., 2023. Arsenic trioxide impairs primary human NK cell responses against influenza A virus. *J. Pharmacol. Exp. Ther.* 385. <https://doi.org/10.1124/jpet.122.208480>.
- Cardoso, A.P.F., Al-Eryani, L., States, J.C., 2018. Arsenic-induced carcinogenesis: the impact of miRNA dysregulation. *Toxicol. Sci. Off. J. Soc. Toxicol.* 165, 284–290. <https://doi.org/10.1093/toxsci/kfy128>.
- Cecchetto, M., Peruzza, L., Giubilato, E., Bernardini, I., Rovere, G.D., Marcomini, A., Regoli, F., Bargelloni, L., Patarnello, T., Semenzin, E., Milan, M., 2023. An innovative index to incorporate transcriptomic data into weight of evidence approaches for environmental risk assessment. *Environ. Res.* 227, 115745. <https://doi.org/10.1016/j.envres.2023.115745>.
- Chain, E.P. on C. in the F., Schrenk, D., Bignami, M., Bodin, L., Chipman, J.K., del Mazo, J., Grasl-Kraupp, B., Hogstrand, C., Hoogenboom, L. (Ron), Leblanc, J.-C., Nebbia, C. S., Nielsen, E., Ntzani, E., Petersen, A., Sand, S., Vlemminckx, C., Wallace, H., Barregård, L., Benford, D., Broberg, K., Dogliotti, E., Fletcher, T., Rylander, L., Abrahamantes, J.C., Gómez Ruiz, J.A., Steinkellner, H., Tauriainen, T., Schwerdtle, T., 2024. Update of the risk assessment of inorganic arsenic in food. *EFSA J.* 22, e8488. doi: 10.2903/j.efsa.2024.8488.
- Chen, B., Khodadoust, M.S., Liu, C.L., Newman, A.M., Alizadeh, A.A., 2018. Profiling tumor infiltrating immune cells with CIBERSORT. *Methods Mol. Biol. Clifton NJ* 1711, 243–259. https://doi.org/10.1007/978-1-4939-7493-1_12.
- Chen, Q.Y., Costa, M., 2018. PI3K/Akt/mTOR signaling pathway and the biphasic effect of arsenic in carcinogenesis. *Mol. Pharmacol.* 94, 784–792. <https://doi.org/10.1124/mol.118.112268>.
- Chen, Q.Y., Shen, S., Sun, H., Wu, F., Kluz, T., Kibriya, M.G., Chen, Y., Ahsan, H., Costa, M., 2020. PBMC gene expression profiles of female Bangladeshi adults chronically exposed to arsenic-contaminated drinking water. *Environ. Pollut. Barking Essex 1987 (259)*, 113672. <https://doi.org/10.1016/j.envpol.2019.113672>.
- Chien, C.-W., Chiang, M.-C., Ho, I.-C., Lee, T.-C., 2004. Association of chromosomal alterations with arsenite-induced tumorigenicity of human HaCaT keratinocytes in nude mice. *Environ. Health Perspect.* 112, 1704. <https://doi.org/10.1289/ehp.7224>.
- Clarke, K., Ainsworth, M., 1993. A method of linking multivariate community structure to environmental variables. *Mar. Ecol. Prog. Ser.* 92, 205–219. <https://doi.org/10.3354/meps092205>.
- De Loma, J., Gliga, A.R., Levi, M., Ascuí, F., Gardon, J., Tirado, N., Broberg, K., 2020. Arsenic exposure and cancer-related proteins in urine of indigenous Bolivian women. *Front. Public Health* 8. <https://doi.org/10.3389/fpubh.2020.605123>.
- De Loma, J., Kraiss, A.M., Lindh, C.H., Mamani, J., Tirado, N., Gardon, J., Broberg, K., 2022a. Arsenic exposure and biomarkers for oxidative stress and telomere length in indigenous populations in Bolivia. *Ecotoxicol. Environ. Saf.* 231, 113194. <https://doi.org/10.1016/j.ecoenv.2022.113194>.
- De Loma, J., Tirado, N., Ascuí, F., Levi, M., Vahter, M., Broberg, K., Gardon, J., 2019. Elevated arsenic exposure and efficient arsenic metabolism in indigenous women around Lake Poopó, Bolivia. *Sci. Total Environ.* 657, 179–186. <https://doi.org/10.1016/j.scitotenv.2018.11.473>.
- De Loma, J., Vicente, M., Tirado, N., Ascuí, F., Vahter, M., Gardon, J., Schlebusch, C.M., Broberg, K., 2022b. Human adaptation to arsenic in Bolivians living in the Andes. *Chemosphere* 301, 134764. <https://doi.org/10.1016/j.chemosphere.2022.134764>.
- Debnath, J., Gammoh, N., Ryan, K.M., 2023. Autophagy and autophagy-related pathways in cancer. *Nat. Rev. Mol. Cell Biol.* 24, 560–575. <https://doi.org/10.1038/s41580-023-00585-z>.
- Dheeman, D.S., Packianathan, C., Pillai, J.K., Rosen, B.P., 2014. Pathway of human AS3MT arsenic methylation. *Chem. Res. Toxicol.* 27, 1979–1989. <https://doi.org/10.1021/tx500313k>.
- Drobná, Z., Del Razo, L.M., García-Vargas, G.G., Sánchez-Peña, L.C., Barrera-Hernández, A., Stýblo, M., Loomis, D., 2013. Environmental exposure to arsenic,

- AS3MT polymorphism and prevalence of diabetes in Mexico. *J. Exposure Sci. Environ. Epidemiol.* 23, 151–155. <https://doi.org/10.1038/jes.2012.103>.
- Engström, K., Vahter, M., Mlakar, S.J., Concha, G., Nermell, B., Raqib, R., Cardozo, A., Broberg, K., 2011. Polymorphisms in arsenic(+III oxidation state) methyltransferase (AS3MT) predict gene expression of AS3MT as well as arsenic metabolism. *Environ. Health Perspect.* 119, 182–188. <https://doi.org/10.1289/ehp.1002471>.
- Engström, K., Wojdacz, T.K., Marabita, F., Ewels, P., Källner, M., Vezzi, F., Prezza, N., Gruselius, J., Vahter, M., Broberg, K., 2017. Transcriptomics and methylomics of CD4-positive T cells in arsenic-exposed women. *Arch. Toxicol.* 91, 2067–2078. <https://doi.org/10.1007/s00204-016-1879-4>.
- Engström, K.S., Hossain, M.B., Lauss, M., Ahmed, S., Raqib, R., Vahter, M., Broberg, K., 2013. Efficient arsenic metabolism—the AS3MT haplotype is associated with DNA methylation and expression of multiple genes around AS3MT. *PLoS One* 8, e53732. <https://doi.org/10.1371/journal.pone.0053732>.
- Engström, K.S., Vahter, M., Fletcher, T., Leonardi, G., Goessler, W., Gurzau, E., Koppova, K., Rudnai, P., Koppova, P., Kumar, R., Broberg, K., 2015. Genetic variation in arsenic (+3 oxidation state) methyltransferase (AS3MT), arsenic metabolism and risk of basal cell carcinoma in a European population. *Environ. Mol. Mutagen.* 56, 60–69. <https://doi.org/10.1002/em.21896>.
- Félix Garza, Z.C., Lenz, M., Liebmann, J., Ertaylan, G., Born, M., Arts, I.C.W., Hilbers, P. A.J., van Riel, N.A.W., 2019. Characterization of disease-specific cellular abundance profiles of chronic inflammatory skin conditions from deconvolution of biopsy samples. *BMC Med. Genomics* 12, 121. <https://doi.org/10.1186/s12920-019-0567-7>.
- Ferrario, D., Gribaldo, L., Hartung, T., 2016. Arsenic exposure and immunotoxicity: a review including the possible influence of age and sex. *Curr. Environ. Health Rep.* 3, 1–12. <https://doi.org/10.1007/s40572-016-0082-3>.
- Ferreccio, C., Smith, A.H., Durán, V., Barlaro, T., Benítez, H., Valdés, R., Aguirre, J.J., Moore, L.E., Acevedo, J., Vásquez, M.I., Pérez, L., Yuan, Y., Liaw, J., Cantor, K.P., Steinmaus, C., 2013. Case-control study of arsenic in drinking water and kidney cancer in uniquely exposed northern Chile. *Am. J. Epidemiol.* 178, 813–818. <https://doi.org/10.1093/aje/kwt059>.
- Freedman, A.N., Hartwell, H., Fry, R., 2025. Using transcriptomic signatures to elucidate individual and mixture effects of inorganic arsenic and manganese in human placental trophoblast HTR-8/SVneo cells. *Toxicol. Sci.* 203, 216–226. <https://doi.org/10.1093/toxsci/afae147>.
- Fry, R.C., Navasumrit, P., Valiathan, C., Svensson, J.P., Hogan, B.J., Luo, M., Bhattacharya, S., Kandjanapa, K., Soontararuks, S., Nookabkaew, S., Mahidol, C., Ruchirawat, M., Samson, L.D., 2007. Activation of inflammation/NF- κ B signaling in infants born to arsenic-exposed mothers. *PLoS Genet.* 3, e207. <https://doi.org/10.1371/journal.pgen.0030207>.
- Fusella, F., Secli, L., Busso, E., Krepelova, A., Moiso, E., Rocca, S., Conti, L., Annaratone, L., Rubinetto, C., Mello-Grand, M., Singh, V., Chiorino, G., Silengo, L., Altruda, F., Turco, E., Morotti, A., Oliviero, S., Castellano, I., Cavallo, F., Provero, P., Tarone, G., Brancaccio, M., 2017. The IKK/NF- κ B signaling pathway requires Morgana to drive breast cancer metastasis. *Nat. Commun.* 8, 1636. <https://doi.org/10.1038/s41467-017-01829-1>.
- Gao, J., Roy, S., Tong, L., Argos, M., Jasmine, F., Rahaman, R., Rakibuz-Zaman, M., Parvez, F., Ahmed, A., Hore, S.K., Sarwar, G., Slavkovich, V., Yunus, M., Rahman, M., Baron, J.A., Graziano, J.H., Ahsan, H., Pierce, B.L., 2015. Arsenic exposure, telomere length, and expression of telomere-related genes among Bangladeshi individuals. *Environ. Res.* 136, 462–469. <https://doi.org/10.1016/j.envres.2014.09.040>.
- Germolec, D.R., Yoshida, T., Gaido, K., Wilmer, J.L., Simeonova, P.P., Kayama, F., Burleson, F., Dong, W., Lange, R.W., Luster, M.I., 1996. Arsenic induces overexpression of growth factors in human keratinocytes. *Toxicol. Appl. Pharmacol.* 141, 308–318. <https://doi.org/10.1006/taap.1996.0288>.
- Greenacre, M., Groenen, P.J.F., Hastie, T., D'Enza, A.I., Markos, A., Tuzhilina, E., 2022. Principal component analysis. *Nat. Rev. Methods Primers* 2, 1–21. <https://doi.org/10.1038/s43586-022-00184-w>.
- Jiang, J., Wang, Y., 2022. Quantitative assessment of arsenite-induced perturbation of ubiquitinated proteome. *Chem. Res. Toxicol.* 35, 1589–1597. <https://doi.org/10.1021/acs.chemrestox.2c00197>.
- Jiang, P., Hou, Z., Bolin, J.M., Thomson, J.A., Stewart, R., 2017. RNA-seq of human neural progenitor cells exposed to lead (Pb) reveals transcriptome dynamics, splicing alterations and disease risk associations. *Toxicol. Sci. Off. J. Soc. Toxicol.* 159, 251–265. <https://doi.org/10.1093/toxsci/kfx129>.
- Juan, W.-S., Mu, Y.-F., Wang, C.-Y., So, E.-C., Lee, Y.-P., Lin, S.-C., Huang, B.-M., 2023. Arsenic compounds activate MAPK and inhibit Akt pathways to induce apoptosis in MA-10 mouse Leydig tumor cells. *Cancer Med.* 12, 3260–3275. <https://doi.org/10.1002/cam4.5068>.
- Kibriya, M.G., Jasmine, F., Munoz, A., Islam, T., Ahmed, A., Tong, L., Rakibuz-Zaman, M., Shahriar, M., Kamal, M., Shea, C.R., Graziano, J.H., Argos, M., Ahsan, H., 2022. Interaction of arsenic exposure and transcriptomic profile in basal cell carcinoma. *Cancers* 14, 5598. <https://doi.org/10.3390/cancers14225598>.
- Kolde, R., 2018. pheatmap: Pretty Heatmaps.
- Kozul, C.D., Hampton, T.H., Davey, J.C., Gosse, J.A., Nomikos, A.P., Eisenhauer, P.L., Weiss, D.J., Thorpe, J.E., Ihnat, M.A., Hamilton, J.W., 2009. Chronic exposure to arsenic in the drinking water alters the expression of immune response genes in mouse lung. *Environ. Health Perspect.* 117, 1108–1115. <https://doi.org/10.1289/ehp.0800199>.
- Lau, A., Zheng, Y., Tao, S., Wang, H., Whitman, S.A., White, E., Zhang, D.D., 2013. Arsenic inhibits autophagic flux, activating the Nrf2-Keap1 pathway in a p62-dependent manner. *Mol. Cell Biol.* 33, 2436. <https://doi.org/10.1128/MCB.01748-12>.
- Li, A., Barber, R.F., 2019. Multiple testing with the structure-adaptive Benjamini-Hochberg algorithm. *J. R. Stat. Soc. Ser. B Stat. Methodol.* 81, 45–74. <https://doi.org/10.1111/rssb.12298>.
- Li, H., Engström, K., Vahter, M., Broberg, K., 2012. Arsenic exposure through drinking water is associated with longer telomeres in peripheral blood. *Chem. Res. Toxicol.* 25, 2333–2339. <https://doi.org/10.1021/tx300222t>.
- Li, Y., Zhang, Z., Jiang, S., Xu, F., Tulum, L., Li, K., Liu, S., Li, S., Chang, L., Liddell, M., Tu, F., Gu, X., Carmichael, P.L., White, A., Peng, S., Zhang, Q., Li, J., Zuo, T., Kucik, P., Xu, P., 2023. Using transcriptomics, proteomics and phosphoproteomics as new approach methodology (NAM) to define biological responses for chemical safety assessment. *Chemosphere* 313, 137359. <https://doi.org/10.1016/j.chemosphere.2022.137359>.
- Lindberg, A.-L., Kumar, R., Goessler, W., Thirumaran, R., Gurzau, E., Koppova, K., Rudnai, P., Leonardi, G., Fletcher, T., Vahter, M., 2007. Metabolism of low-dose inorganic arsenic in a central European population: influence of sex and genetic polymorphisms. *Environ. Health Perspect.* <https://doi.org/10.1289/ehp.10026>.
- Liu, L., Liu, Q., 2024. Characterization of macrophages in head and neck squamous cell carcinoma and development of MRG-based risk signature. *Sci. Rep.* 14, 9914. <https://doi.org/10.1038/s41598-024-60516-6>.
- Liu, Q., Li, P., Ma, J., Zhang, J., Li, W., Liu, Y., Liu, L., Liang, S., He, M., 2024. Arsenic exposure at environmentally relevant levels induced metabolic toxicity in development mice: mechanistic insights from integrated transcriptome and metabolome. *Environ. Int.* 190, 108819. <https://doi.org/10.1016/j.envint.2024.108819>.
- Love, M.I., Huber, W., Anders, S., 2014. Moderated estimation of fold change and dispersion for RNA-seq data with DESeq2. *Genome Biol.* 15, 550. <https://doi.org/10.1186/s13059-014-0550-8>.
- Ministerio de Medio Ambiente y Agua, Viceministerio de Agua Potable y Saneamiento Básico, 2018. Compendio Normativo sobre Calidad de Agua para Consumo Humano NB 512 - Reglamento NB 512 - NB 495 - NB496. Instituto Boliviano de Normalización y Calidad IBNORCA, La Paz, Bolivia.
- Moon, K., Guallar, E., Navas-Acien, A., 2012. Arsenic exposure and cardiovascular disease: an updated systematic review. *Curr. Atheroscler. Rep.* 14, 542–555. <https://doi.org/10.1007/s11883-012-0280-x>.
- Muhetaer, M., Yang, M., Xia, R., Lai, Y., Wu, J., 2022. Gender difference in arsenic biotransformation is an important metabolic basis for arsenic toxicity. *BMC Pharmacol. Toxicol.* 23, 15. <https://doi.org/10.1186/s40360-022-00554-w>.
- Ozturk, H., Cingöz, H., Tufan, T., Yang, J., Adair, S.J., Tummala, K.S., Kuscü, C., Kinali, M., Comertpay, G., Nagdas, S., Goudreau, B.J., Luleyp, H.U., Bingül, Y., Ware, T.B., Hwang, W.L., Hsu, K., Kashatus, D.F., Ting, D.T., Chandel, N.S., Bardeesy, N., Bauer, T.W., Adli, M., 2022. ISL2 is a putative tumor suppressor whose epigenetic silencing reprograms the metabolism of pancreatic cancer. *Dev. Cell* 57, 1331–1346.e9. <https://doi.org/10.1016/j.devcel.2022.04.014>.
- Peng, Y., Wang, Y., Zhou, C., Mei, W., Zeng, C., 2022. PI3K/Akt/mTOR pathway and its role in cancer therapeutics: are we making headway? *Front. Oncol.* 12, 819128. <https://doi.org/10.3389/fonc.2022.819128>.
- Pierce, B.L., Kibriya, M.G., Tong, L., Jasmine, F., Argos, M., Roy, S., Paul-Brutus, R., Rahaman, R., Rakibuz-Zaman, M., Parvez, F., Ahmed, A., Quasem, I., Hore, S.K., Alam, S., Islam, T., Slavkovich, V., Gamble, M.V., Yunus, M., Rahman, M., Baron, J.A., Graziano, J.H., Ahsan, H., 2012. Genome-wide association study identifies chromosome 10q24.32 variants associated with arsenic metabolism and toxicity phenotypes in Bangladesh. *PLoS Genet.* 8, e1002522. <https://doi.org/10.1371/journal.pgen.1002522>.
- Podgorski, J., Berg, M., 2020. Global threat of arsenic in groundwater. *Science* 368, 845–850. <https://doi.org/10.1126/science.aba1510>.
- Poggio, P., Rocca, S., Fusella, F., Ferretti, R., Ala, U., D'Anna, F., Giugliano, E., Panuzzo, C., Fontana, D., Palumbo, V., Carrà, G., Taverna, D., Gambacorti-Passerini, C., Saglio, G., Fava, C., Piazza, R., Morotti, A., Orso, F., Brancaccio, M., 2024. miR-15a targets the HSP90 co-chaperone Morgana in chronic myeloid leukemia. *Sci. Rep.* 14, 15089. <https://doi.org/10.1038/s41598-024-65404-7>.
- Qi, Y., Zhang, M., Li, H., Frank, J.A., Dai, L., Liu, H., Zhang, Z., Wang, C., Chen, G., 2014. Autophagy inhibition by sustained overproduction of IL6 contributes to arsenic carcinogenesis. *Cancer Res.* 74, 3740–3752. <https://doi.org/10.1158/0008-5472.CAN-13-3182>.
- Rehman, M.Y.A., van Herwijnen, M., Krauskopf, J., Farooqi, A., Kleinjans, J.C.S., Malik, R.N., Briedé, J.J., 2020. Transcriptome responses in blood reveal distinct biological pathways associated with arsenic exposure through drinking water in rural settings of Punjab, Pakistan. *Environ. Int.* 135, 105403. <https://doi.org/10.1016/j.envint.2019.105403>.
- Reverendo, M., Argüello, R.J., Polte, C., Valečka, J., Camosseto, V., Auphan-Anezin, N., Ignatova, Z., Gatti, E., Pierre, P., 2019. Polymerase III transcription is necessary for T cell priming by dendritic cells. *PNAS* 116, 22721–22729. <https://doi.org/10.1073/pnas.1904396116>.
- Shukla, V., Chandrasekaran, B., Tyagi, A., Navin, A.K., Saran, U., Adam, R.M., Damodaran, C., 2022. A comprehensive transcriptomic analysis of arsenic-induced bladder carcinogenesis. *Cells* 11, 2435. <https://doi.org/10.3390/cells11152435>.
- Smoot, M.E., Ono, K., Ruscheinski, J., Wang, P.-L., Ideker, T., 2011. Cytoscape 2.8: new features for data integration and network visualization. *Bioinform. Oxf. Engl.* 27, 431–432. <https://doi.org/10.1093/bioinformatics/btq675>.
- Sprenger, H., Kreuzer, K., Alarcán, J., Herrmann, K., Buchmüller, J., Marx-Stoelting, P., Braeuning, A., 2022. Use of transcriptomics in hazard identification and next generation risk assessment: a case study with clothianidin. *Food Chem. Toxicol. Int. J. Publ. Br. Ind. Biol. Res. Assoc.* 166, 113212. <https://doi.org/10.1016/j.fct.2022.113212>.
- Stråvik, M., Gustin, K., Barman, M., Levi, M., Sandin, A., Wold, A.E., Sandberg, A.-S., Kippler, M., Vahter, M., 2023. Biomarkers of seafood intake during pregnancy –

- pollutants versus fatty acids and micronutrients. *Environ. Res.* 225, 115576. <https://doi.org/10.1016/j.envres.2023.115576>.
- Sumi, D., Tsuyama, H., Ogawa, T., Ogawa, M., Himeno, S., 2021. Arsenite suppresses IL-2-dependent tumoricidal activities of natural killer cells. *Toxicol. Appl. Pharmacol.* 412, 115353. <https://doi.org/10.1016/j.taap.2020.115353>.
- Szklarczyk, D., Gable, A.L., Lyon, D., Junge, A., Wyder, S., Huerta-Cepas, J., Simonovic, M., Doncheva, N.T., Morris, J.H., Bork, P., Jensen, L.J., von Mering, C., 2019. STRING v11: protein–protein association networks with increased coverage, supporting functional discovery in genome-wide experimental datasets. *Nucleic Acids Res.* 47, D607–D613. <https://doi.org/10.1093/nar/gky1131>.
- Tam, L.M., Price, N.E., Wang, Y., 2020. Molecular mechanisms of arsenic-induced disruption of DNA repair. *Chem. Res. Toxicol.* 33, 709–726. <https://doi.org/10.1021/acs.chemrestox.9b00464>.
- Tang, G.T., Elakis, J., Scardamaglia, L., 2023. Cutaneous manifestations and treatment of arsenic toxicity: a systematic review. *Skin Health Dis.* 3, e231. <https://doi.org/10.1002/ski2.231>.
- Tchounwou, P.B., Udensi, U.K., Isokpehi, R.D., Yedjou, C.G., Kumar, S., 2023. Arsenic and cancer. In: Flora, S.J.S. (Ed.), *Handbook of Arsenic Toxicology* (second Edition), 23. Academic Press, Oxford, pp. 607–630. <https://doi.org/10.1016/B978-0-323-89847-8.00018-3>.
- Tirado, N., Mamani, J., De Loma, J., Ascui, F., Broberg, K., Gardon, J., 2024. Genotoxicity in humans exposed to arsenic, lithium, and boron in drinking water in the Bolivian Andes—a cross sectional study. *Environ. Mol. Mutagen.* 65, 121–128. <https://doi.org/10.1002/em.22587>.
- Torbøl Pedersen, J., De Loma, J., Levi, M., Palmgren, M., Broberg, K., 2020. Predicted AS3MT proteins methylate arsenic and support two major phylogenetic AS3MT groups. *Chem. Res. Toxicol.* 33, 3041–3047. <https://doi.org/10.1021/acs.chemrestox.0c00375>.
- Trouba, K.J., Glanzer, J.G., Vorce, R.L., 1999. Wild-type and Ras-transformed fibroblasts display differential mitogenic responses to transient sodium arsenite exposure. *Toxicol. Sci. Off. J. Soc. Toxicol.* 50, 72–81. <https://doi.org/10.1093/toxsci/50.1.72>.
- Tsou, T.-C., Tsai, F.-Y., Hsieh, Y.-W., Li, L.-A., Yeh, S.C., Chang, L.W., 2005. Arsenite induces endothelial cytotoxicity by down-regulation of vascular endothelial nitric oxide synthase. *Toxicol. Appl. Pharmacol.* 208, 277–284. <https://doi.org/10.1016/j.taap.2005.03.001>.
- Vahter, M., 1999. Variation in Human Metabolism of Arsenic. In: Chappell, W.R., Abernathy, C.O., Calderon, R.L. (Eds.), *Arsenic Exposure and Health Effects III*. Elsevier Science Ltd, Oxford, pp. 267–279. <https://doi.org/10.1016/B978-008043648-7/50031-5>.
- Vahter, M., Åkesson, A., Lidén, C., Ceccatelli, S., Berglund, M., 2007. Gender differences in the disposition and toxicity of metals. *Environ. Res., Scientific Group on Methodologies for the Safety Evaluation of Chemicals: Workshop 16—Gender Differences and Human and Ecological Risk* 104, 85–95. doi: 10.1016/j.envres.2006.08.003.
- Vega, L., Styblo, M., Patterson, R., Cullen, W., Wang, C., Germolec, D., 2001. Differential effects of trivalent and pentavalent arsenicals on cell proliferation and cytokine secretion in normal human epidermal keratinocytes. *Toxicol. Appl. Pharmacol.* 172, 225–232. <https://doi.org/10.1006/taap.2001.9152>.
- Water, N.R.C. (US) S. on A. in D., 1999. Biomarkers of Arsenic Exposure, in: *Arsenic in Drinking Water*. National Academies Press (US).
- Wu, J., Ni, Y., Yang, Q., Mao, J., Zhu, X., Tao, S., Kato, K., Zhang, J., Wang, D., Yamanaka, K., An, Y., 2020. Long-term arsenite exposure decreases autophagy by increased release of Nrf2 in transformed human keratinocytes. *Sci. Total Environ.* 734, 139425. <https://doi.org/10.1016/j.scitotenv.2020.139425>.
- Xie, H., Huang, S., Martin, S., Wise, J.P., 2014. Arsenic is cytotoxic and genotoxic to primary human lung cells. *Mutat. Res. Genet. Toxicol. Environ. Mutagen.* 760, 33–41. <https://doi.org/10.1016/j.mrgentox.2013.11.001>.
- Xie, L., Hu, W.-Y., Hu, D.-P., Shi, G., Li, Y., Yang, J., Prins, G.S., 2020. Effects of inorganic arsenic on human prostate stem-progenitor cell transformation, autophagic flux blockade, and NRF2 pathway activation. *Environ. Health Perspect.* 128, 067008. <https://doi.org/10.1289/EHP6471>.
- Yamada, H., Uenishi, R., Suzuki, K., Koizumi, S., 2009. Cadmium-induced alterations of gene expression in human cells. *Environ. Toxicol. Pharmacol.* 28, 61–69. <https://doi.org/10.1016/j.etap.2009.02.007>.
- Yang, Y., Chen, X., Deng, L., Huang, Y., Mo, Y., Ye, J., Liang, R., Qin, Y., Zhang, Q., Wang, S., 2025. Arsenic exposure provoked prostatic PANoptosis by inducing mitochondrial dysfunction in mice and WPMY-1 cells. *Ecotoxicol. Environ. Saf.* 295, 118139. <https://doi.org/10.1016/j.ecoenv.2025.118139>.
- Yu, G., Wang, L.-G., Han, Y., He, Q.-Y., 2012. clusterProfiler: an R package for comparing biological themes among gene clusters. *Omics J. Integr. Biol.* 16, 284–287. <https://doi.org/10.1089/omi.2011.0118>.
- Zhang, Z., Xiong, X., Zhang, R., Xiong, G., Yu, C., Xu, L., 2021. Bioinformatics analysis reveals biomarkers with cancer stem cell characteristics in kidney renal clear cell carcinoma. *Transl. Androl. Urol.* 10, 3501–3514. <https://doi.org/10.21037/tau-21-647>.